

Nonconvex Stochastic Bregman Proximal Gradient Method with Application to Deep Learning

Kuangyu Ding

Department of Mathematics

University of Singapore

10 Lower Kent Ridge Road, Singapore 119076

KUANGYUD@U.NUS.EDU

Jingyang Li

Department of Mathematics

University of Singapore

10 Lower Kent Ridge Road, Singapore 119076

LLJINGYANG@U.NUS.EDU

Kim-Chuan Toh

Department of Mathematics Institute of Operations Research and Analytics

University of Singapore

10 Lower Kent Ridge Road, Singapore 119076

MATTOHKC@NUS.EDU.SG

Editor:

Abstract

The widely used stochastic gradient methods for minimizing nonconvex composite objective functions require the Lipschitz smoothness of the differentiable part. But the requirement does not hold true for problem classes including quadratic inverse problems and training neural networks. To address this issue, we investigate a family of stochastic Bregman proximal gradient (SBPG) methods, which only require smooth adaptivity of the differentiable part. SBPG replaces the upper quadratic approximation used in SGD with the Bregman proximity measure, resulting in a better approximation model that captures the non-Lipschitz gradients of the nonconvex objective. We formulate the vanilla SBPG and establish its convergence properties under nonconvex setting without finite-sum structure. Experimental results on quadratic inverse problems testify the robustness of SBPG. Moreover, we propose a momentum-based version of SBPG (MSBPG) and prove it has improved convergence properties. We apply MSBPG to the training of deep neural networks with a polynomial kernel function, which ensures the smooth adaptivity of the loss function. Experimental results on representative benchmarks demonstrate the effectiveness and robustness of MSBPG in training neural networks. Since the additional computation cost of MSBPG compared with SGD is negligible in large-scale optimization, MSBPG can potentially be employed as an universal open-source optimizer in the future.

Keywords: Nonconvex stochastic algorithm, Bregman distance, Smooth adaptivity, Deep neural network, Gradient explosion

1. Introduction

In this paper, we present and analyze a family of nonconvex stochastic Bregman proximal gradient methods (SBPG) for solving the following generic stochastic minimization problem:

$$\min_{\mathbf{x} \in \mathcal{C}} \mathbb{E}_{\boldsymbol{\xi}} [f(\mathbf{x}, \boldsymbol{\xi})] + R(\mathbf{x}), \quad (1)$$

where $f(\cdot, \boldsymbol{\xi})$ is a nonconvex differentiable function on \overline{C} , R is a proper lower-semicontinuous convex function, $\boldsymbol{\xi}$ is a random variable, and \overline{C} is the closure of C , which is a nonempty convex open subset of \mathbb{R}^d . We denote $F(\mathbf{x}) := \mathbb{E}_{\boldsymbol{\xi}}[f(\mathbf{x}, \boldsymbol{\xi})]$, and $\Phi(\mathbf{x}) := F(\mathbf{x}) + R(\mathbf{x})$. This stochastic minimization problem, where an optimizer has limited access to the distribution of $\boldsymbol{\xi}$ and can only draw samples from it, is prevalent in the fields of machine learning and statistics (Hastie et al., 2009; Shapiro et al., 2021; Zhang, 2004). In many instances, the smooth part of the objective function $F(\mathbf{x})$ can be formulated as a finite-sum structure $F(\mathbf{x}) = \frac{1}{n} \sum_{i=1}^n f_i(\mathbf{x})$. However, when n is extremely large, calculating the true gradient for the smooth part of the objective function becomes extremely expensive. As a result, stochastic first-order methods, which trace back to the work of Robbins and Monro (1951), have become the prevailing approach for solving these large-scale optimization problems. In particular, stochastic (proximal) gradient descent and its numerous variants (Duchi et al., 2011; Duchi and Singer, 2009; Gu et al., 2020; Kingma and Ba, 2014; Allen-Zhu, 2018; Wang et al., 2022) have been widely utilized in large-scale stochastic optimization for machine learning (LeCun et al., 2015; Shapiro et al., 2021; Zhang, 2004). From modeling perspective, stochastic gradient descent can be viewed as minimizing a sequence of upper quadratic approximations of the nonconvex objective $\Phi(\mathbf{x})$:

$$\mathbf{x}^{k+1} = \operatorname{argmin}_{\mathbf{x} \in \overline{C}} \left\{ \underbrace{F(\mathbf{x}^k, \boldsymbol{\Xi}_k) + \langle \widetilde{\nabla}_k, \mathbf{x} - \mathbf{x}^k \rangle + \frac{1}{2\alpha_k} \|\mathbf{x} - \mathbf{x}^k\|^2 + R(\mathbf{x})}_{F_{\mathbf{x}^k}(\mathbf{x}): \text{model of } F \text{ at } \mathbf{x}^k} \right\}, \quad (2)$$

where $F(\mathbf{x}^k, \boldsymbol{\Xi}_k) := \frac{1}{|\boldsymbol{\Xi}_k|} \sum_{\boldsymbol{\xi} \in \boldsymbol{\Xi}_k} f(\mathbf{x}^k, \boldsymbol{\xi})$, $\boldsymbol{\Xi}_k$ is the set of samples of $\boldsymbol{\xi}$ at the k -th iteration, and $\widetilde{\nabla}_k$ is an estimator of the exact gradient $\nabla F(\mathbf{x}^k)$. This modeling perspective is well-known in deterministic optimization, and has been used in methods such as Newton method, Gauss-Newton method, bundle methods, and trust-region methods, as discussed in various sources such as Hiriart-Urruty and Lemaréchal (1993); Nesterov (2003); Lin et al. (2007); Paren et al. (2022).

Despite being widely used, stochastic gradient methods (2) still have several well-known bottlenecks both in theory and practice. One of the crucial requirements for analyzing stochastic gradient methods is the assumption of Lipschitz continuity of the gradient of the differentiable part, which is essential for ensuring the convergence of the algorithm. However, this assumption does not always hold true. For example, even the seemingly simple function $F(x) = x^4$ does not admit a globally Lipschitz gradient over \mathbb{R} , which highlights the challenges of analyzing stochastic gradient methods. In addition, choosing the appropriate stepsize is another challenge in the practical usage of stochastic gradient methods. The stepsize has a significant impact on the convergence performance of the algorithm, and finding the optimal stepsize can be a time-consuming process. Engineers may have to conduct multiple experiments to determine the optimal stepsize, further compounding the complexity of the problem at hand.

To address these issues, classical approaches often resort to either line search or more complicated inner loops, but these methods can negatively impact the efficiency of the algorithm or even becomes intractable in a stochastic setting. For instance, stochastic proximal point algorithm (PPA) model the approximation of $F(\mathbf{x})$ in (2) as $F_{\mathbf{x}^k}(\mathbf{x}) =$

$F(\mathbf{x}, \boldsymbol{\xi}_k) + \frac{1}{2\alpha_k} \|\mathbf{x} - \mathbf{x}^k\|^2$ (Bertsekas, 2011; Bianchi, 2016; Patrascu and Necoara, 2017; Rockafellar, 1976), which makes the selection of stepsize α_k more robust than the original model (2). However, the application of stochastic PPA is limited due to the difficulty of solving the subproblems, particularly when dealing with complicated objective functions, such as training deep neural networks. In such cases, solving the subproblem is almost as difficult as solving the original problem, rendering the approach impractical. Recently, Bauschke et al. (2017); Lu et al. (2018) have proposed using Bregman proximity measures to relax the assumption of gradient Lipschitz continuity to smooth adaptivity. The Bregman gradient method was first introduced as the mirror descent scheme by Nemirovskij and Yudin (1983) for minimizing convex nonsmooth functions. From the modeling perspective, Bregman methods consider the following subproblem at each iteration:

$$\mathbf{x}^{k+1} = \operatorname{argmin}_{\mathbf{x} \in \bar{C}} \left\{ \underbrace{F(\mathbf{x}^k, \boldsymbol{\Xi}_k) + \langle \tilde{\nabla}_k, \mathbf{x} - \mathbf{x}^k \rangle + \frac{1}{\alpha_k} \mathcal{D}_\phi(\mathbf{x}, \mathbf{x}^k) + R(\mathbf{x})}_{F_{\mathbf{x}^k}(\mathbf{x}): \text{model of } F \text{ at } \mathbf{x}^k} \right\}, \quad (3)$$

where \mathcal{D}_ϕ is the Bregman distance induced by the kernel function ϕ . To convey the advantage of the Bregman proximity model, we present a toy example. Consider objective function $F(x) = x^4$ with non-Lipschitz gradient continuity, we compare the effectiveness of the upper quadratic approximation model (2) and Bregman proximity model (3). As apparent from Figure (1)(a), the Bregman proximity model (3) ($F_2(x)$) with the kernel function $\phi(x) = \frac{1}{2}x^2 + \frac{1}{4}x^4$ can provide a more suitable approximation for $F(x)$ than the upper quadratic approximation model 2 ($F_1(x)$), as the yellow curve stays closer to the curve of the objective function $F(x) = x^4$. With this improved approximation, x^{k+1} generated by the Bregman gradient method can make more significant progress towards approaching the optimal solution ($x^* = 0$) than x^{k+1} generated by the gradient descent method, as depicted in Figure 1(b).

While several stochastic extensions of Bregman methods that are based on smooth adaptivity assumption have been developed recently, the current literature primarily focuses on stochastic convex problems (Dragomir et al., 2021b; Hanzely and Richtárik, 2021; Lu, 2019). The only existing convergence analysis of Bregman methods for nonconvex problems (Latafat et al., 2022) requires a finite-sum structure and a novel equivalent consensus reformulation. Moreover, it is memory-intensive and requires essentially periodic computation of the full gradient, which is expensive for large-scale problems such as deep neural networks (Defazio and Bottou, 2019). As we can see, stochastic Bregman methods have not been fully explored in the context of modern large-scale nonconvex problems such as training neural networks, and rigorous numerical evaluations of their performance are limited. Furthermore, current literature lacks attention towards the robustness of stochastic Bregman methods, particularly in terms of selecting stepsizes and initial points, which can significantly impact their performance in large-scale problems.

In this paper, we consider stochastic Bregman proximal gradient methods (SBPG) for nonconvex problems (without finite-sum structure requirement) with application to the training of deep neural networks. We establish the convergence result of a vanilla SBPG without Lipschitz smoothness assumption for nonconvex problems. Moreover, we propose a

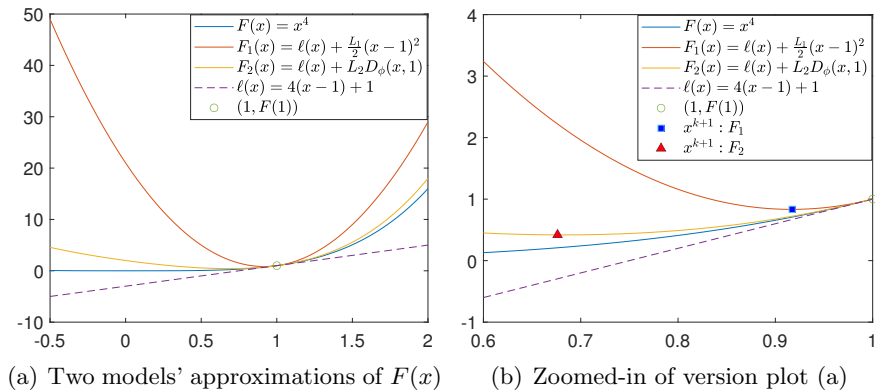


Figure 1: For function $F(x) = x^4$, which does not admit a globally Lipschitz continuous gradient. We restrict the feasible set to $[-0.5, 2]$. Consider the models (2) and (3) of F at $x^k = 1$. The Lipschitz constant of F with respect to the kernel $\phi(x) = \frac{1}{2}x^2$ is 48. The Lipschitz constant of F with respect to the kernel $\phi(x) = \frac{1}{2}x^2 + \frac{1}{4}x^4$ is 4. The figure in (b) is a zoomed-in version of the plot in (a) for the range $[0.6, 1]$. The unique minimum of $F(x)$ is at $x = 0$.

momentum-based SBPG (denoted as MSBPG) and prove that it has improved convergence properties compared with vanilla SBPG. We apply MSBPG to the training of deep neural networks with a polynomial kernel function, which ensures the smooth adaptivity of the loss function. According to our analysis, MSBPG can improve the robustness of training neural networks by mitigating the gradient explosion phenomenon and improve generalization performance by adopting Bregman proximity approximation to the loss function locally. For numerical illustrations, we conduct numerical experiments on quadratic inverse problems (QIP) and testify vanilla SBPG’s robustness to stepsize selection and initial point’s scaling. We also conduct extensive experiments on training CNNs for image classification and LSTMs for language modeling by employing MSBPG, which is well-suited for solving large-scale problems. Experimental results on representative benchmarks show that our MSBPG has excellent generalization performance, outperforming the most frequently used optimization algorithms, including SGD (Robbins and Monro, 1951), Adam (Kingma and Ba, 2014), and AdamW (Loshchilov and Hutter, 2017). Furthermore, MSBPG is demonstrated to be robustness to large stepsize and initial point’s scaling, which are the common reasons behind gradient explosion.

To summarize, our contributions are as follows:

1. We investigate Stochastic Bregman Proximal Gradient (SBPG) method to solve non-convex problem without finite-sum requirement, which employs Bregman distance to handle the non-Lipschitz gradient continuity. We establish convergence results for the vanilla SBPG in the sense of expectation. Further, we propose a momentum-based SBPG (MSBPG) that is tailored for modern large-scale applications, and prove that it has improved convergence properties compared to the vanilla SBPG. To our best

knowledge, this is the first time that the momentum technique has been integrated into a stochastic Bregman proximal gradient method.

2. We apply MSBPG to training deep neural networks (DNN), which leverages on a suitable polynomial kernel function to ensure that the DNN’s loss function is smooth adaptable with respect to the designed kernel function. MSBPG exhibits good convergence behavior and excellent generalization performance on extensive tasks. Moreover, MSBPG is found to be more robust than the traditional SGD, especially when it comes to stepsize selection and initialization. We highlight that MSBPG is a theoretically derived method that is able to ease the difficulty of selecting stepsize, mitigate gradient explosion, and maintains excellent generalization performance simultaneously. This distinguishes MSBPG from many existing techniques that rely on intuition and empirical observations.
3. We demonstrate the efficiency and robustness of SBPG or MSBPG in a range of applications, including sparse quadratic inverse problems and large-scale deep neural networks. In quadratic inverse problem, SBPG is more robust in terms of both stepsize and initial point selections. In training deep neural networks, MSBPG has been found to achieve a superior generalization performance compared with some of the most frequently used optimizers such as Adam and AdamW, and also exhibits robustness to stepsize selection and initialization. These results highlight the potential of MSBPG as a powerful tool for optimizing complex and large-scale deep neural networks, thus offering a promising direction for future research in this area.

The remainder of this paper is organized as follows. In Section 2, we present notation, some related preliminaries and our problem setting. In Section 3, we first describe SBPG and establish its convergence results in the sense of expectation. Then, we propose a momentum-based SBPG (MSBPG) and prove its improved convergence properties. In Section 4, we adapt MSBPG to the training of deep neural networks and analyze its capacity in mitigating gradient explosion and improving generalization capacity. In Section 5, we present numerical experiments that demonstrate the efficiency and robustness of vanilla SBPG on quadratic inverse problems and MSBPG on training deep neural networks. Finally, we give some concluding remarks in Section 6, summarizing our key contributions and outlining promising topics for future research.

2. Preliminaries and Problem setting

In this paper, vectors are represented using boldface letters like \mathbf{v} , while scalars are represented using normal font. Given a proper, lower-semicontinuous function $F : \mathbb{R}^d \rightarrow \bar{\mathbb{R}} := [-\infty, \infty]$, $\text{dom } F = \{\mathbf{x} : F(\mathbf{x}) < \infty\}$. The Fenchel conjugate function of F is defined as $F^*(\mathbf{y}) = \sup\{\langle \mathbf{x}, \mathbf{y} \rangle - F(\mathbf{x}) : \mathbf{x} \in \mathbb{R}^d\}$. Given a set $\mathcal{S} \subset \mathbb{R}^d$, $\bar{\mathcal{S}}$ denotes its closure, $\text{int } \mathcal{S}$ denotes the set of interior points. A function is of class $\mathcal{C}^k(\mathcal{S})$ if it is k times differentiable and the k -th derivative is continuous on \mathcal{S} . We say that F is level bounded if the set $\{\mathbf{x} : F(\mathbf{x}) < \alpha\}$ is bounded for any real number α . Given a matrix A , $\text{Vec}(A)$ denotes the vectorization of A by column order. $\text{Mat}(\cdot)$ is the inverse operation of $\text{Vec}(\cdot)$, which reshapes a vector back into its original matrix form. Define the operator $\text{Diag}(\cdot)$ to map a

vector into a diagonal matrix with diagonal elements equal to the corresponding entries of the vector. The Hadamard product is represented by the symbol \circ . If we use the notation $\|\cdot\|$ without any additional explanation, we assume that it refers to the Euclidean vector norm for vectors and the Frobenius matrix norm for matrices.

Let $(\Omega, \mathcal{F}, \mathbb{P})$ be a probability space. Given a random variable $\boldsymbol{\xi}$ and a σ -algebra \mathcal{F} , we write $\boldsymbol{\xi} \triangleleft \mathcal{F}$ if $\boldsymbol{\xi}$ is measurable over \mathcal{F} . Let $\{\boldsymbol{\xi}_k\}_{k \geq 0}$ be a stochastic process, and $\{\mathcal{F}_k\}_{k \geq 0}$ be a filtration, where \mathcal{F}_k defined by a σ -algebra $\mathcal{F}_k := \sigma(\boldsymbol{\xi}_0, \dots, \boldsymbol{\xi}_{k-1})$ on Ω . The conditional expectation is denoted by $\mathbb{E}[\cdot | \mathcal{F}_k]$. For simplicity, we use the notation $\mathbb{E}[\cdot]$ to denote $\mathbb{E}[\cdot | \mathcal{F}_\infty]$. The sequence $\{\mathbf{x}^k\}_{k \geq 0}$ generated by our proposed method is adapted to the filtration $\{\mathcal{F}_k\}_{k \geq 0}$, i.e. $\mathbf{x}^k \triangleleft \mathcal{F}_k$, for all $k \geq 0$. The notation $\tilde{\nabla}_k$ represents an estimator of the exact gradient $\nabla F(\mathbf{x}^k)$, which satisfies $\tilde{\nabla}_k \triangleleft \mathcal{F}_{k+1}$. This estimator is applicable to both the vanilla and momentum cases. The stochastic error is denoted by $\boldsymbol{\varepsilon}_k = \nabla F(\mathbf{x}^k) - \tilde{\nabla}_k$. The unbiasedness of the stochastic error $\boldsymbol{\varepsilon}_k$ is assumed throughout this paper, i.e., $\mathbb{E}[\boldsymbol{\varepsilon}_k | \mathcal{F}_k] = 0$. The following supermartingale convergence theorem is a fundamental tool in the analysis of stochastic algorithms.

Theorem 1 (*Robbins and Monro, 1951*) *Let $\{y_k\}, \{u_k\}, \{a_k\}$ and $\{b_k\}$ be non-negative adapted processes with respect to the filtration $\{\mathcal{F}_k\}$ such that $\sum_k a_k < \infty, \sum_k b_k < \infty$, and for all $k, \mathbb{E}[y_{k+1} | \mathcal{F}_k] \leq (1 + a_k)y_k - u_k + b_k$ almost surely. Then, $\{y_k\}$ converges almost surely to a non-negative finite random variable and $\sum_k u_k < \infty$ almost surely.*

2.1 Smooth adaptable functions

In this subsection, we introduce the concept of smooth adaptivity, which was initially proposed in Bolte et al. (2018). This concept is an extension of the idea of relative smoothness for convex functions introduced in Bauschke et al. (2017); Lu et al. (2018). We first give the definitions of kernel function and Bregman distance.

Definition 2 (*Kernel function and Bregman distance*). *Let \mathcal{S} be a nonempty, convex and open subset of \mathbb{R}^d . Associated with \mathcal{S} , a function $\phi : \mathbb{R}^d \rightarrow (-\infty, +\infty]$ is called a kernel function if it satisfies the following two conditions:*

1. ϕ is proper, lower-semicontinuous and convex, with $\text{dom } \phi \subset \bar{\mathcal{S}}, \text{dom } \partial \phi = \mathcal{S}$.
2. $\phi \in \mathcal{C}^1(\mathcal{S})$ and $\text{int dom } \phi = \mathcal{S}$.

Denote the class of kernel function associated with \mathcal{S} by $\mathcal{M}(\mathcal{S})$. Given $\phi \in \mathcal{M}(\mathcal{S})$, the Bregman distance (Bregman, 1967) generated by ϕ is defined as $\mathcal{D}_\phi(\mathbf{x}, \mathbf{y}) : \text{dom } \phi \times \text{int dom } \phi \rightarrow [0, +\infty)$, where

$$\mathcal{D}_\phi(\mathbf{x}, \mathbf{y}) = \phi(\mathbf{x}) - \phi(\mathbf{y}) - \langle \nabla \phi(\mathbf{y}), \mathbf{x} - \mathbf{y} \rangle.$$

Bregman distance measures the difference between the value of ϕ at \mathbf{x} and its linear approximation at \mathbf{y} based on the gradient of ϕ at \mathbf{y} . Some basic properties of Bregman distance can be found in Chen and Teboulle (1993); Teboulle (2018). Some kernel functions commonly used in optimization are $\frac{1}{2}\|\mathbf{x}\|^2, \frac{1}{2}\|\mathbf{x}\|^2 + \frac{\alpha}{4}\|\mathbf{x}\|^4, -\sum_{i=1}^d \log \mathbf{x}_i$ and $\sum_{i=1}^d \mathbf{x}_i \log \mathbf{x}_i$, where $\frac{1}{2}\|\mathbf{x}\|^2 \in \mathcal{M}(\mathbb{R}^d)$ recovers the classical half squared Euclidean distance. The kernel function $\frac{1}{2}\|\mathbf{x}\|^2 + \frac{\alpha}{4}\|\mathbf{x}\|^4 \in \mathcal{M}(\mathbb{R}^d)$ has found applications in various problems, such as quadratic inverse problems, non-negative matrix factorization, and low-rank minimization (Bolte et al.,

2018; Dragomir et al., 2021a). The entropy function $\sum_{i=1}^d \mathbf{x}_i \log \mathbf{x}_i \in \mathcal{M}(\mathbb{R}_{++}^d)$ is commonly used in applications that involve probability constraints, where the resulting Bregman distance is known as the Kullback–Leibler (KL) divergence. Throughout the paper we will focus on the following pair of functions (f, ϕ) satisfying smooth adaptivity condition. We introduce this concept in the following definition:

Definition 3 (*Smooth adaptivity*). *Given a kernel function $\phi \in \mathcal{M}(\mathcal{S})$, a proper lower-semicontinuous function $f : \mathbb{R}^d \rightarrow (-\infty, +\infty]$ with $\text{dom } f \supset \text{dom } \phi$ that is \mathcal{C}^1 on \mathcal{S} . f is L -smooth adaptable with respect to ϕ if there exists $L > 0$, such that $L\phi + f$ and $L\phi - f$ are convex on \mathcal{S} .*

Alternative definition of smooth adaptivity is the two-side descent lemma (Bolte et al., 2018, Lemma 2.1). When both f and ϕ belong to $\mathcal{C}^2(\mathcal{S})$, we can verify their smooth adaptivity by comparing the Hessians of f and ϕ .

Lemma 4 *f is L -smooth adaptable with respect to $\phi \in \mathcal{M}(\mathcal{S})$, if and only if*

$$|f(\mathbf{x}) - f(\mathbf{y}) - \langle \nabla f(\mathbf{y}), \mathbf{x} - \mathbf{y} \rangle| \leq L\mathcal{D}_\phi(\mathbf{x}, \mathbf{y}), \quad \forall \mathbf{x}, \mathbf{y} \in \text{int dom } \phi.$$

Moreover, when both f and ϕ belong to $\mathcal{C}^2(\text{int dom } \phi)$, then the above is equivalent to

$$\exists L > 0, L\nabla^2\phi(\mathbf{x}) - \nabla^2f(\mathbf{x}) \succeq 0, \quad \text{for all } \mathbf{x} \in \text{int dom } \phi.$$

The following four-point identity is frequently employed in our proofs, and can be easily verified.

Lemma 5 (*Four points identity*) *Given points $\mathbf{a}, \mathbf{b}, \mathbf{c}, \mathbf{d}$ and any convex function ϕ which is differentiable at \mathbf{a} and \mathbf{b} , then*

$$\langle \nabla\phi(\mathbf{a}) - \nabla\phi(\mathbf{b}), \mathbf{c} - \mathbf{d} \rangle = \mathcal{D}_\phi(\mathbf{c}, \mathbf{b}) + \mathcal{D}_\phi(\mathbf{d}, \mathbf{a}) - \mathcal{D}_\phi(\mathbf{c}, \mathbf{a}) - \mathcal{D}_\phi(\mathbf{d}, \mathbf{b}).$$

2.2 Bregman Proximal Mapping

Throughout this paper, we make the following basic assumptions.

Assumption 1 (*Basic requirements*). *In problem (1):*

- A1. For every fixed ξ , $f(\cdot, \xi)$ is a proper lower-semicontinuous function with $\text{dom } \phi \subset \text{dom } f(\cdot, \xi)$, and it is \mathcal{C}^1 on $\text{int } C$.
- A2. The Legendre kernel (Definition 6) $\phi \in \mathcal{M}(C)$ is μ -strongly convex for some $\mu > 0$. For every fixed ξ , $f(\cdot, \xi)$ is L_F -smooth adaptable with respect to ϕ , where L_F is independent of ξ .
- A3. R is a proper, lower semicontinuous and convex function with $\text{dom } R \cap \text{int } C \neq \emptyset$.
- A4. $\inf_{\mathbf{x} \in \overline{C}} \{\Phi(\mathbf{x})\} > -\infty$.

Assumption 1 is a standard requirement for Bregman-type methods and is usually satisfied in practice. It ensures the well-definedness of Bregman-type methods, as shown in Bolte et al. (2018); Latafat et al. (2022). We also recall the definition of the Legendre function in Latafat et al. (2022), which makes additional supercoercive conditions on the concept in Rockafellar (1997).

Definition 6 (*Legendre kernel*). Let $\phi : \bar{C} \rightarrow (-\infty, \infty]$ be a proper lower-semicontinuous convex function. It is called essentially smooth if $\text{int dom } \phi$ is nonempty and ϕ is differentiable on $\text{int dom } \phi$, moreover $\lim_{k \rightarrow \infty} \|\nabla \phi(\mathbf{x}^k)\| = \infty$ whenever $\{\mathbf{x}^k\}_{k \in \mathbb{N}}$ converges to a boundary point of $\text{dom } \phi$. The function ϕ is called Legendre function if it is essentially smooth, strictly convex on $\text{int dom } \phi$ and supercoercive, i.e. $\lim_{\|\mathbf{x}\| \rightarrow \infty} \frac{\phi(\mathbf{x})}{\|\mathbf{x}\|} = \infty$.

Definition 7 Given a nonempty convex open set C , a proper lower-semicontinuous convex function R and a Legendre kernel function $\phi \in \mathcal{M}(C)$, $\mathbf{x} \in \text{int } \phi$, we denote the Bregman proximal mapping by $\text{Prox}_R^\phi := (\nabla \phi + \partial R)^{-1} \nabla \phi$, which is defined as

$$\text{Prox}_R^\phi(\mathbf{x}) := \underset{\mathbf{u} \in \bar{C}}{\text{argmin}} \{R(\mathbf{u}) + \mathcal{D}_\phi(\mathbf{u}, \mathbf{x})\}. \quad (4)$$

Note that the objective function of (4) is strictly convex on $\text{dom } \phi \cap \text{dom } R$, therefore (4) has at most one solution. To ensure that (4) is well-defined, the following result claims that $\text{Prox}_{\alpha R}^\phi(\mathbf{x})$ is well-defined for any $\alpha > 0$, and moreover $\text{Prox}_{\alpha R}^\phi(\mathbf{x}) \in \text{int dom } \phi$ under standard assumptions. The proof can be found in Appendix A.

Lemma 8 *Suppose Assumption 1 holds. Then (4) has a unique solution. Moreover, the solution $\text{Prox}_{\alpha R}^\phi(\mathbf{x}) \in C$.*

The following proposition for Bregman proximal mapping generalizes the nonexpansive property of the classical proximal mapping (in the case $\phi(\mathbf{x}) = \frac{1}{2}\|\mathbf{x}\|^2$). This property is commonly used in convergence proofs. The proof of the following proposition can be found in Appendix A.

Proposition 9 *Suppose Assumption 1 holds. Let $\mathbf{x}_i^+ := \text{Prox}_R^\phi(\nabla \phi^*(\mathbf{x}_i))$, $i = 1, 2$. Then $\|\mathbf{x}_1^+ - \mathbf{x}_2^+\| \leq \frac{1}{\mu} \|\mathbf{x}_1 - \mathbf{x}_2\|$.*

In this paper, we make the assumption that R and ϕ are simple enough so that (4) either has a closed-form solution or admits an efficient subroutine to solve it. Using the definition of the Bregman proximal mapping, we can then define the Bregman gradient mapping associated with (1). This mapping measures the solution accuracy of the methods we propose. Note that ϕ is a Legendre kernel, which implies that $\phi^* \in \mathcal{C}^1(\mathbb{R}^d)$ is strictly convex and $(\nabla \phi)^{-1} = \nabla \phi^*$ (Rockafellar, 1997, Corollary 13.3.1, Theorem 26.5). Therefore, the following concept is well-defined.

Definition 10 (Bregman Gradient Mapping) *Given $\alpha > 0$, a nonempty convex open set C and a Legendre kernel function $\phi \in \mathcal{M}(C)$, the Bregman gradient mapping associated with (1) is defined as follows*

$$\mathcal{G}_\alpha(\mathbf{x}) = \frac{\mathbf{x} - \text{Prox}_{\alpha R}^\phi(\nabla \phi^*(\nabla \phi(\mathbf{x}) - \alpha \nabla F(\mathbf{x})))}{\alpha}.$$

To simplify notation, we use $\mathcal{G}(\mathbf{x})$ to denote $\mathcal{G}_1(\mathbf{x})$ when $\alpha = 1$.

When the kernel function $\phi(\mathbf{x}) = \frac{1}{2}\|\mathbf{x}\|^2$, the resulting Bregman Gradient Mapping becomes equivalent to the classical Gradient Mapping (Nesterov, 2003, 2005), which measures the solution’s accuracy for proximal gradient methods.

Definition 11 (*Limiting subdifferential (Rockafellar and Wets, 1998, Definition 8.3)*) Consider a function $f : \mathbb{R}^d \rightarrow \bar{\mathbb{R}}$ and a point x , the regular subdifferential is defines as

$$\hat{\partial}f(\mathbf{x}) = \{\mathbf{v} : f(\mathbf{y}) \geq f(\mathbf{x}) + \langle \mathbf{v}, \mathbf{y} - \mathbf{x} \rangle + o(\|\mathbf{y} - \mathbf{x}\|)\}.$$

The limiting subdifferential is defined as

$$\partial f(\mathbf{x}) = \{\mathbf{v} : \mathbf{x}_n \rightarrow \mathbf{x}, f(\mathbf{x}_n) \rightarrow f(\mathbf{x}), \mathbf{v}_n \in \hat{\partial}f(\mathbf{x}_n), \text{ and } \mathbf{v}_n \rightarrow \mathbf{v}\}.$$

By Fermat’s rule (Rockafellar and Wets, 1998, Theorem 10.1), the set of critical point of Φ is given by

$$\text{crit } \Phi = \left\{x \in \mathbb{R}^d : 0 \in \partial\Phi(x) \equiv \nabla F(x) + \partial R(x)\right\}.$$

The Bregman Gradient Mapping can also be used to evaluate the solution accuracy for Bregman methods. Let $\mathbf{x}^+ = \text{Prox}_{\alpha R}^{\phi}(\nabla\phi^*(\nabla\phi(\mathbf{x}) - \alpha\nabla F(\mathbf{x})))$. From Definition 10 and equation (4), it can be easily verified by definition that $0 \in \partial\Phi(\mathbf{x}) \Leftrightarrow 0 = \mathcal{G}_{\alpha}(\mathbf{x})$. Hence, $0 \in \partial\Phi(\mathbf{x}^+)$ for any $\alpha > 0$. The proof of this result is omitted for brevity. Furthermore, if $\nabla\phi$ is L_{ϕ} -Lipschitz continuous, then the following proposition holds, implying that $\|\mathcal{G}_{\alpha}(\mathbf{x})\|$ can be used as a reasonable criterion to measure the accuracy of \mathbf{x} .

Proposition 12 *Suppose Assumption 1 holds and that $\nabla\phi$ is L_{ϕ} Lipschitz continuous. Then, we have the following inequality:*

$$\text{dist}(0, \partial\Phi(\mathbf{x}^+)) \leq (1 + \alpha L_F)L_{\phi}\|\mathcal{G}_{\alpha}(\mathbf{x})\|.$$

We also define the stochastic counterpart of Definition 10, which is commonly utilized to evaluate the accuracy of solutions for nonconvex stochastic proximal gradient methods, as discussed in Ghadimi et al. (2016).

Definition 13 (*Stochastic Bregman Gradient Mapping*). Given $\alpha > 0$ a nonempty convex open set C and a Legendre kernel function $\phi \in \mathcal{M}(C)$, the stochastic Bregman gradient mapping associated with (1) is defined as follows

$$\tilde{\mathcal{G}}_{\alpha}(\mathbf{x}) := \frac{\mathbf{x} - \text{Prox}_{\alpha R}^{\phi}\left(\nabla\phi^*\left(\nabla\phi(\mathbf{x}) - \alpha\tilde{\nabla}\right)\right)}{\alpha}, \text{ where } \tilde{\nabla} \text{ is an estimator of } \nabla F(\mathbf{x}).$$

3. Stochastic Bregman Proximal Gradient Method

In this section, we will study the Stochastic Bregman Proximal Gradient method (SBPG) with the following update scheme:

$$\mathbf{x}^{k+1} = \underset{\mathbf{x} \in \bar{C}}{\text{argmin}} R(\mathbf{x}) + \langle \tilde{\nabla}_k, \mathbf{x} - \mathbf{x}^k \rangle + \frac{1}{\alpha_k} \mathcal{D}_{\phi}(\mathbf{x}, \mathbf{x}^k). \quad (5)$$

We call the above method as "vanilla" SBPG in this section, meaning that the method we study is a basic version without any additional techniques such as variance reduction, momentum, etc., except for the use of mini-batches. In this case, we suppose the following assumptions.

Assumption 2 (Noise requirement). *The estimator satisfies the following two conditions:*

$$\mathbb{E}[\tilde{\nabla}_k | \mathcal{F}_k] = \nabla F(\mathbf{x}^k) \quad \text{and} \quad \mathbb{E}[\|\tilde{\nabla}_k - \nabla F(\mathbf{x}^k)\|^2 | \mathcal{F}_k] \leq \frac{\sigma^2}{m_k},$$

where m_k is the size of the mini-batch in the k -th iteration.

Note that we do not assume a finite-sum structure for $F(\mathbf{x})$ in this section. The solution of (5) can be written in the form of the Bregman proximal mapping. This is stated in the following proposition.

Proposition 14 *Suppose Assumption 1 holds. Then the solution of (5) can be written as the following Bregman proximal mapping:*

$$\mathbf{x}^{k+1} = \text{Prox}_{\alpha_k R}^{\phi} \left(\nabla \phi^* \left(\nabla \phi(\mathbf{x}^k) - \alpha_k \tilde{\nabla}_k \right) \right).$$

Proof From the optimality condition of the main subproblem (5), we have

$$0 \in \partial R(\mathbf{x}^{k+1}) + \tilde{\nabla}_k + \frac{1}{\alpha_k} \left(\nabla \phi(\mathbf{x}^{k+1}) - \nabla \phi(\mathbf{x}^k) \right).$$

Let $\mathbf{u}^{k+1} := \text{Prox}_{\alpha_k R}^{\phi} \left(\nabla \phi^* \left(\nabla \phi(\mathbf{x}^k) - \alpha_k \tilde{\nabla}_k \right) \right)$. From the definition of Bregman proximal mapping, we have

$$\mathbf{u}^{k+1} = \arg \min_{\mathbf{u}} \left\{ \alpha_k R(\mathbf{u}) + \mathcal{D}_{\phi} \left(\mathbf{u}, \nabla \phi^* \left(\nabla \phi(\mathbf{x}^k) - \alpha_k \tilde{\nabla}_k \right) \right) \right\},$$

which is equivalent to

$$0 \in \alpha_k \partial R(\mathbf{u}^{k+1}) + \nabla \phi(\mathbf{u}^{k+1}) - \nabla \phi(\nabla \phi^* (\nabla \phi(\mathbf{x}^k) - \alpha_k \tilde{\nabla}_k)).$$

Note that the function ϕ^* is the Fenchel conjugate of the Legendre kernel ϕ , which implies that $\nabla \phi(\nabla \phi^*(\mathbf{w})) = \mathbf{w}$ for all $\mathbf{w} \in \mathbb{R}^d$, as stated in (Rockafellar, 1997, Corollary 13.3.1, Theorem 26.5). Furthermore, since the objective function in (5) is strictly convex, there exists a unique solution to the inclusion above. By comparing the two inclusions, we can conclude that $\mathbf{u}^{k+1} = \mathbf{x}^{k+1}$. \blacksquare

Based on Proposition 14 and definition of the definition of $\tilde{\mathcal{G}}_{\alpha}(\mathbf{x})$, we can easily observe that $\mathbf{x}^{k+1} = \mathbf{x}^k - \alpha_k \tilde{\mathcal{G}}_{\alpha_k}(\mathbf{x}^k)$. We can derive the following proposition, which bounds the difference between $\mathcal{G}_{\alpha}(\mathbf{x})$ and $\tilde{\mathcal{G}}_{\alpha}(\mathbf{x})$ directly from Proposition 9. The proof is omitted for brevity.

Proposition 15 *Suppose Assumption 1 holds. At the k -th step, we have the estimation:*

$$\|\mathcal{G}_{\alpha_k}(\mathbf{x}^k) - \tilde{\mathcal{G}}_{\alpha_k}(\mathbf{x}^k)\| \leq \frac{1}{\mu} \|\nabla F(\mathbf{x}^k) - \tilde{\nabla}_k\| = \frac{\|\boldsymbol{\varepsilon}_k\|}{\mu},$$

where $\boldsymbol{\varepsilon}_k = \nabla F(\mathbf{x}^k) - \tilde{\nabla}_k$.

Before presenting the main convergence result, we state the following one-step descent lemma below.

Lemma 16 *Suppose Assumption 1 holds. The sequence generated by SBPG satisfies the following condition:*

$$\Phi(\mathbf{x}^{k+1}) \leq \Phi(\mathbf{x}^k) - \frac{1}{\alpha_k} \mathcal{D}_\phi(\mathbf{x}^k, \mathbf{x}^{k+1}) - \left(\frac{1}{\alpha_k} - L_F \right) \mathcal{D}_\phi(\mathbf{x}^{k+1}, \mathbf{x}^k) + \langle \boldsymbol{\varepsilon}_k, \mathbf{x}^{k+1} - \mathbf{x}^k \rangle.$$

Proof By the optimality condition of (5), we obtain that

$$0 \in \partial R(\mathbf{x}^{k+1}) + \tilde{\nabla}_k + \frac{1}{\alpha_k} \left(\nabla \phi(\mathbf{x}^{k+1}) - \nabla \phi(\mathbf{x}^k) \right).$$

Appealing to the convexity of R , we have

$$R(\mathbf{x}) - R(\mathbf{x}^{k+1}) \geq \langle -\tilde{\nabla}_k - \frac{1}{\alpha_k} \left(\nabla \phi(\mathbf{x}^{k+1}) - \nabla \phi(\mathbf{x}^k) \right), \mathbf{x} - \mathbf{x}^{k+1} \rangle.$$

By the four points identity and the definition of $\boldsymbol{\varepsilon}_k$, we get

$$R(\mathbf{x}) - R(\mathbf{x}^{k+1}) \geq \frac{1}{\alpha_k} \left[\mathcal{D}_\phi(\mathbf{x}^{k+1}, \mathbf{x}^k) + \mathcal{D}_\phi(\mathbf{x}, \mathbf{x}^{k+1}) - \mathcal{D}_\phi(\mathbf{x}, \mathbf{x}^k) \right] - \langle \nabla F(\mathbf{x}^k), \mathbf{x} - \mathbf{x}^{k+1} \rangle + \langle \boldsymbol{\varepsilon}_k, \mathbf{x} - \mathbf{x}^{k+1} \rangle.$$

Set $\mathbf{x} = \mathbf{x}^k$ in the above inequality, we have the following inequality:

$$R(\mathbf{x}^k) - R(\mathbf{x}^{k+1}) \geq \frac{1}{\alpha_k} \left[\mathcal{D}_\phi(\mathbf{x}^{k+1}, \mathbf{x}^k) + \mathcal{D}_\phi(\mathbf{x}^k, \mathbf{x}^{k+1}) \right] - \langle \nabla F(\mathbf{x}^k), \mathbf{x}^k - \mathbf{x}^{k+1} \rangle + \langle \boldsymbol{\varepsilon}_k, \mathbf{x}^k - \mathbf{x}^{k+1} \rangle.$$

By the smooth adaptivity of F , we have

$$F(\mathbf{x}^{k+1}) \leq F(\mathbf{x}^k) + \langle \nabla F(\mathbf{x}^k), \mathbf{x}^{k+1} - \mathbf{x}^k \rangle + L_F \mathcal{D}_\phi(\mathbf{x}^{k+1}, \mathbf{x}^k).$$

Combining the above two inequalities above, we complete the proof. ■

3.1 Convergence analysis of SBPG

In this subsection, we establish the convergence results for SBPG, which is an extension of the convergence result in Ghadimi et al. (2016), in which the lassical Lipschitz gradient assumption is required. In many literature, the bounded sequence assumption is often required in the convergence analysis of stochastic algorithms. However, in this section, we relax this assumption and prove that under a certain condition, the sequence generated by (5) is bounded almost surely. We need the following result to bound the stochastic error term $\langle \boldsymbol{\varepsilon}_k, \mathbf{x}^{k+1} - \mathbf{x}^k \rangle$ in Lemma 16.

Lemma 17 *Suppose Assumption 1, 2 hold. We have the following estimation of the error term:*

$$\mathbb{E} \left[\langle \boldsymbol{\varepsilon}_k, \mathbf{x}^{k+1} - \mathbf{x}^k \rangle \right] \leq \frac{\alpha_k}{\mu} \mathbb{E} [\| \boldsymbol{\varepsilon}_k \|^2] \leq \frac{\alpha_k \sigma^2}{\mu m_k}.$$

Proof Define $\bar{\mathbf{x}}^{k+1} := \text{Prox}_{\alpha_k R}^{\phi}(\nabla\phi^*(\nabla\phi(\mathbf{x}^k) - \alpha_k \nabla F(\mathbf{x}^k)))$. By Proposition 14 and the optimality condition for $\bar{\mathbf{x}}^{k+1}$, we have

$$0 \in \partial R(\bar{\mathbf{x}}^{k+1}) + \nabla F(\mathbf{x}^k) + \frac{1}{\alpha_k}(\nabla\phi(\bar{\mathbf{x}}^{k+1}) - \nabla\phi(\mathbf{x}^k)).$$

Similarly,

$$0 \in \partial R(\mathbf{x}^{k+1}) + \tilde{\nabla}_k + \frac{1}{\alpha_k}(\nabla\phi(\mathbf{x}^{k+1}) - \nabla\phi(\mathbf{x}^k)).$$

By the monotonicity of ∂R and Lemma 5, we have

$$\langle \bar{\mathbf{x}}^{k+1} - \mathbf{x}^{k+1}, -\varepsilon_k - \frac{1}{\alpha_k}(\nabla\phi(\bar{\mathbf{x}}^{k+1}) - \nabla\phi(\mathbf{x}^{k+1})) \rangle \geq 0.$$

Therefore,

$$\langle \mathbf{x}^{k+1} - \bar{\mathbf{x}}^{k+1}, \varepsilon_k \rangle \geq \langle \bar{\mathbf{x}}^{k+1} - \mathbf{x}^{k+1}, \frac{1}{\alpha_k}(\nabla\phi(\bar{\mathbf{x}}^{k+1}) - \nabla\phi(\mathbf{x}^{k+1})) \rangle \geq \frac{\mu}{\alpha_k} \|\bar{\mathbf{x}}^{k+1} - \mathbf{x}^{k+1}\|^2.$$

By Cauchy-Schwarz inequality, we get $\|\bar{\mathbf{x}}^{k+1} - \mathbf{x}^{k+1}\| \leq \frac{\alpha_k}{\mu} \|\varepsilon_k\|$.

Now, we are ready to prove Lemma 17. From the definition, we know that $\bar{\mathbf{x}}^{k+1} \triangleleft \mathcal{F}_k$. Therefore, $\mathbb{E}[\langle \varepsilon_k, \mathbf{x}^k - \bar{\mathbf{x}}^{k+1} \rangle] = \mathbb{E}[\mathbb{E}[\langle \varepsilon_k, \mathbf{x}^k - \bar{\mathbf{x}}^{k+1} \rangle | \mathcal{F}_k]] = \mathbb{E}[\langle \mathbb{E}[\varepsilon_k | \mathcal{F}_k], \mathbf{x}^k - \bar{\mathbf{x}}^{k+1} \rangle] = 0$, where the first equality is from the tower rule of conditional expectation, the second comes from the fact that $\mathbf{x}^k - \bar{\mathbf{x}}^{k+1} \triangleleft \mathcal{F}_k$. Hence,

$$\mathbb{E}[\langle \varepsilon_k, \mathbf{x}^{k+1} - \mathbf{x}^k \rangle] = \mathbb{E}[\langle \varepsilon_k, \mathbf{x}^{k+1} - \bar{\mathbf{x}}^{k+1} \rangle] - \mathbb{E}[\langle \varepsilon_k, \mathbf{x}^k - \bar{\mathbf{x}}^{k+1} \rangle] \leq \frac{\alpha_k}{\mu} \mathbb{E}[\|\varepsilon_k\|^2] \leq \frac{\alpha_k \sigma^2}{\mu m_k},$$

which completes the proof. \blacksquare

Lemma 18 (Bounded sequence) *Suppose Assumption 1, 2 hold. If $\sum_k \frac{\alpha_k}{m_k} < \infty$, $\sup_k \alpha_k \leq \bar{\alpha} < \frac{1}{L_F}$, then,*

1. $\sum_{k=0}^{\infty} \mathbb{E}[\mathcal{D}_{\phi}(\mathbf{x}^{k+1}, \mathbf{x}^k)] < \infty$.
2. If Φ is level bounded, then $\{\mathbf{x}^k\}_{k \geq 0}$ is bounded almost surely.

Proof By Cauchy-Young inequality, we have

$$|\langle \varepsilon_k, \mathbf{x}^k - \mathbf{x}^{k+1} \rangle| \leq \frac{\mu}{2\alpha_k} \|\mathbf{x}^k - \mathbf{x}^{k+1}\|^2 + \frac{\alpha_k}{2\mu} \|\varepsilon_k\|^2 \leq \frac{1}{\alpha_k} \mathcal{D}_{\phi}(\mathbf{x}^k, \mathbf{x}^{k+1}) + \frac{\alpha_k}{2\mu} \|\varepsilon_k\|^2.$$

By Lemma 16, we have

$$\left(\frac{1}{\alpha_k} - L_F \right) \mathcal{D}_{\phi}(\mathbf{x}^{k+1}, \mathbf{x}^k) \leq \Phi(\mathbf{x}^k) - \Phi(\mathbf{x}^{k+1}) + \frac{\alpha_k}{2\mu} \|\varepsilon_k\|^2. \quad (6)$$

Taking conditional expectation for both sides of (6), we get

$$\mathbb{E} \left[\left(\frac{1}{\alpha_k} - L_F \right) \mathcal{D}_{\phi}(\mathbf{x}^{k+1}, \mathbf{x}^k) | \mathcal{F}_k \right] \leq \Phi(\mathbf{x}^k) - \mathbb{E}[\Phi(\mathbf{x}^{k+1}) | \mathcal{F}_k] + \frac{\alpha_k}{2\mu} \mathbb{E}[\|\varepsilon_k\|^2 | \mathcal{F}_k].$$

Since $\sum_{k \geq 0} \frac{\alpha_k}{2\mu} \mathbb{E}[\|\varepsilon_k\|^2 | \mathcal{F}_k] \leq \sum_{k \geq 0} \frac{\alpha_k \sigma^2}{2\mu m_k} < \infty$, applying Theorem 1, we have that $\Phi(\mathbf{x}^k)$ converges and $\sum_{k \geq 0} \mathbb{E} \left[\left(\frac{1}{\alpha_k} - L_F \right) \mathcal{D}_\phi(\mathbf{x}^{k+1}, \mathbf{x}^k) | \mathcal{F}_k \right] < \infty$ almost surely. By the tower rule of conditional expectation, we have $\sum_{k=0}^{\infty} \mathbb{E}[\mathcal{D}_\phi(\mathbf{x}^{k+1}, \mathbf{x}^k)] < \infty$. Since $\Phi(\mathbf{x}^k)$ converges almost surely, thus $\{\Phi(\mathbf{x}^k)\}_{k \geq 0}$ is bounded almost surely. By the level boundness of Φ , we deduce that $\{\mathbf{x}^k\}_{k \geq 0}$ is bounded almost surely. \blacksquare

Now, we present our main convergence result for the vanilla SBPG, which is in the sense of expectation.

Theorem 19 (Convergence result in expectation) *Suppose Assumption 1, 2 hold, $\alpha_k < \frac{1}{L_F} \min\{1, \frac{1}{\mu}\}$. Define a random variable r with the distribution $\mathbb{P}\{r = k\} = \frac{\alpha_k}{\sum_{k=0}^{N-1} \alpha_k}$ for $k = 0, \dots, N-1$. Then,*

$$\mathbb{E}[\|\tilde{\mathcal{G}}_{\alpha_r}(\mathbf{x}^r)\|^2] \leq \frac{2\Phi(\mathbf{x}^0) - 2\Phi^* + 2 \sum_{k=0}^{N-1} \frac{\alpha_k \sigma^2}{\mu m_k}}{\mu \sum_{k=0}^{N-1} \alpha_k}. \quad (7)$$

Moreover, if Φ is level bounded, $\sum_k \frac{\alpha_k}{m_k} < +\infty$ and $\sum_k \alpha_k = +\infty$, then the sequence $\{\mathbf{x}^k\}_{k \geq 0}$ is bounded almost surely, and the right hand side of (7) converges to zero.

Proof Note that $\mathbf{x}^{k+1} = \mathbf{x}^k - \alpha_k \tilde{\mathcal{G}}_{\alpha_k}(\mathbf{x}^k)$ and by the strongly convexity of ϕ , Lemma 16 yields

$$\begin{aligned} \mu \left(\alpha_k - \frac{L_F \alpha_k^2}{2} \right) \|\tilde{\mathcal{G}}_{\alpha_k}(\mathbf{x}^k)\|^2 &\leq \frac{1}{\alpha_k} \mathcal{D}_\phi(\mathbf{x}^k, \mathbf{x}^{k+1}) + \left(\frac{1}{\alpha_k} - L_F \right) \mathcal{D}_\phi(\mathbf{x}^{k+1}, \mathbf{x}^k) \\ &\leq \Phi(\mathbf{x}^k) - \Phi(\mathbf{x}^{k+1}) + \langle \varepsilon_k, \mathbf{x}^{k+1} - \mathbf{x}^k \rangle. \end{aligned}$$

Taking expectations, telescoping from $k = 0 \dots N-1$, and using Lemma 17, we obtain

$$\sum_{k=0}^{N-1} \mu \left(\alpha_k - \frac{\mu L_F \alpha_k^2}{2} \right) \mathbb{E}[\|\tilde{\mathcal{G}}_{\alpha_k}(\mathbf{x}^k)\|^2] \leq \Phi(\mathbf{x}^0) - \Phi(\mathbf{x}^N) + \sum_{k=0}^{N-1} \frac{\alpha_k \sigma^2}{\mu m_k}. \quad (8)$$

By utilizing the inequality $\alpha_k - \frac{\mu L_F \alpha_k^2}{2} \geq \frac{\alpha_k}{2}$, the condition $\Phi(\mathbf{x}^N) \geq \Phi^*$, and considering the definition of the random variable r , we can derive (7) from (8). \blacksquare

Remark 20 *We give some remarks for Theorem 19.*

1. *The mini-batch setting is a crucial component for ensuring the convergence, as it allows us to control the stochastic error term in Lemma 16 and provide a bound for $\mathbb{E}[\|\tilde{\mathcal{G}}_{\alpha_k}(\mathbf{x}^k)\|^2]$ that converges to zero as k tends to infinity. If $m_k = 1$ for all k , then the upper bound for $\mathbb{E}[\|\tilde{\mathcal{G}}_{\alpha_k}(\mathbf{x}^k)\|^2]$ will not converge to zero, no matter how $\{\alpha_k\}$ is selected.*

2. In Ghadimi et al. (2016), a similar convergence result is established for nonconvex stochastic proximal gradient methods, but our analysis differs in a crucial aspect in that we do not assume the Lipschitz continuity of $F(\mathbf{x})$. Instead, we assume that $F(\mathbf{x})$ is smooth adaptable, which is a more relaxed assumption. Moreover, we provide a specific choice of stepsizes $\{\alpha_k\}$ and mini-batch sizes $\{m_k\}$ that guarantee the convergence of $\mathbb{E}[\|\tilde{\mathcal{G}}_{\alpha_k}(\mathbf{x}^k)\|^2]$ to 0, as well as the almost sure boundedness of the sequence.

Based on Proposition 15 and Theorem 19, we can derive the following convergence result using the measure $\mathcal{G}_{\alpha_r}(\mathbf{x}^r)$. This can be obtained by observing that $\|\mathcal{G}_{\alpha_r}(\mathbf{x}^r)\|^2 \leq 2\|\tilde{\mathcal{G}}_{\alpha_r}(\mathbf{x}^r)\|^2 + 2\|\mathcal{G}_{\alpha_r}(\mathbf{x}^r) - \tilde{\mathcal{G}}_{\alpha_r}(\mathbf{x}^r)\|^2$.

Corollary 21 *Under the conditions in Theorem 19, we have*

$$\mathbb{E}[\|\mathcal{G}_{\alpha_r}(\mathbf{x}^r)\|^2] \leq \frac{4\Phi(\mathbf{x}^0) - 4\Phi^* + 4 \sum_{k=0}^{N-1} \frac{\alpha_k \sigma^2}{\mu m_k}}{\sum_{k=0}^{N-1} \mu \alpha_k} + \frac{2\sigma^2}{\mu^2 m_k}.$$

3.2 Momentum based Stochastic Bregman Gradient Descent Method

Remark 20 suggests that increasing the mini-batch size m_k is almost necessary for the error bound in Theorem 19 to converge to zero. However, using a large mini-batch size in each iteration can be computationally expensive in the modern large-scale problems, e.g. training deep neural network. In this part, we resort to the momentum technique to address this issue. Specifically, we consider using a stochastic moving average estimator (SMAE) for the true gradient given by:

$$\mathbf{v}^k = (1 - \beta_k)\mathbf{v}^{k-1} + \beta_k \tilde{\nabla}_k, \quad \text{where } \mathbb{E}[\tilde{\nabla}_k | \mathcal{F}_k] = \nabla F(\mathbf{x}^k), \quad (9)$$

where \mathbf{v}^{k-1} can be viewed as the momentum which contain the information of all historical stochastic gradients, and $\mathbb{E}[\|\tilde{\nabla}_k\|^2 | \mathcal{F}_k] \leq \frac{\sigma^2}{m_k}$. We expect that incorporating the SMAE technique can achieve a certain level of variance reduction without increasing the mini-batch size. In our approach, we utilize the gradient estimator \mathbf{v}^k within SBPG, and we refer to the resulting method as MSBPG. Specifically, we consider the following update scheme:

$$\mathbf{x}^{k+1} = \underset{\mathbf{x} \in \mathcal{C}}{\operatorname{argmin}} R(\mathbf{x}) + \langle \mathbf{v}^k, \mathbf{x} - \mathbf{x}^k \rangle + \frac{1}{\alpha_k} \mathcal{D}_\phi(\mathbf{x}, \mathbf{x}^k). \quad (10)$$

We need the following assumption that the difference of gradients of F can be bounded by the Bregman distance.

Assumption 3 *There exists $\kappa > 0$, such that $\|\nabla F(\mathbf{x}) - \nabla F(\mathbf{y})\|^2 \leq \kappa \mathcal{D}_\phi(\mathbf{x}, \mathbf{y})$ for all $\mathbf{x} \in \operatorname{dom} \phi$, $\mathbf{y} \in \operatorname{int} \operatorname{dom} \phi$.*

Remark 22 *This assumption generalizes the case of Lipschitz kernel function. Assume that F is L_F smooth adaptable to ϕ , it can be easily shown that if ϕ has L_ϕ -Lipschitz gradient, this assumption holds for $\kappa \geq \frac{2L_F^2 L_\phi^2}{\mu}$. In this paper, we are more interested in polynomial kernel functions. For functions with polynomially bounded growth rates, this assumption is not restrictive. For example, consider the one-dimensional objective function*

$F(x) = \frac{1}{4}x^4$ and the kernel function $\phi(x) = \frac{1}{2}x^2 + \frac{1}{8}x^8$. Then, by (Lu et al., 2018, Proposition 2.1), we know that F is smooth adaptable with respect to ϕ . Simple algebra shows that $\mathcal{D}_\phi(x, y) = \frac{1}{8}(x-y)^2(x^6 + 2x^5y + 3x^4y^2 + 4x^3y^3 + 5x^2y^4 + 6xy^5 + 7y^6 + 4)$ and $(F'(x) - F'(y))^2 = (x-y)^2(x^2 + xy + y^2)^2$. Numerical computation shows that $(x^6 + 2x^5y + 3x^4y^2 + 4x^3y^3 + 5x^2y^4 + 6xy^5 + 7y^6 + 4) - (x^2 + xy + y^2)^2 \geq 3.71$. Therefore, $(F'(x) - F'(y))^2 \leq 8\mathcal{D}_\phi(x, y)$, which holds globally for any x and y .

Next we present a recursion lemma that allows us to estimate the accuracy of the SMAE. While similar lemmas have been proposed in the literature, such as in Wang et al. (2017), their bounds are not directly applicable in the Bregman setting. As a result, we have developed a version of the recursion lemma that is tailored to our specific context.

Lemma 23 *The following recursion holds*

$$\mathbb{E}[\|\mathbf{v}^k - \nabla F(\mathbf{x}^k)\|^2 | \mathcal{F}_k] \leq (1 - \beta_k) \|\mathbf{v}^{k-1} - \nabla F(\mathbf{x}^{k-1})\|^2 + \beta_k^2 \mathbb{E}[\|\tilde{\nabla}_k - \nabla F(\mathbf{x}^k)\|^2 | \mathcal{F}_k] + \frac{\|\nabla F(\mathbf{x}^{k-1}) - \nabla F(\mathbf{x}^k)\|^2}{\beta_k}.$$

Proof Note that $\mathbf{v}^k - \nabla F(\mathbf{x}^k) = (1 - \beta_k)(\mathbf{v}^{k-1} - \nabla F(\mathbf{x}^{k-1})) + (1 - \beta_k)(\nabla F(\mathbf{x}^{k-1}) - \nabla F(\mathbf{x}^k)) + \beta_k(\tilde{\nabla}_k - \nabla F(\mathbf{x}^k))$, and $\mathbb{E}[\tilde{\nabla}_k - \nabla F(\mathbf{x}^k) | \mathcal{F}_k] = 0$. Then we have

$$\begin{aligned} & \mathbb{E}[\|\mathbf{v}^k - \nabla F(\mathbf{x}^k)\|^2 | \mathcal{F}_k] \\ &= (1 - \beta_k)^2 \|\mathbf{v}^{k-1} - \nabla F(\mathbf{x}^{k-1})\|^2 + (1 - \beta_k)^2 \|\nabla F(\mathbf{x}^{k-1}) - \nabla F(\mathbf{x}^k)\|^2 + \\ & \quad \beta_k^2 \mathbb{E}[\|\tilde{\nabla}_k - \nabla F(\mathbf{x}^k)\|^2 | \mathcal{F}_k] + 2(1 - \beta_k)^2 \langle \mathbf{v}^{k-1} - \nabla F(\mathbf{x}^{k-1}), \nabla F(\mathbf{x}^{k-1}) - \nabla F(\mathbf{x}^k) \rangle \\ &\leq (1 - \beta_k)^2 \|\mathbf{v}^{k-1} - \nabla F(\mathbf{x}^{k-1})\|^2 + (1 - \beta_k)^2 \|\nabla F(\mathbf{x}^{k-1}) - \nabla F(\mathbf{x}^k)\|^2 + \\ & \quad \beta_k^2 \mathbb{E}[\|\tilde{\nabla}_k - \nabla F(\mathbf{x}^k)\|^2 | \mathcal{F}_k] + \beta_k(1 - \beta_k) \|\mathbf{v}^{k-1} - \nabla F(\mathbf{x}^{k-1})\|^2 + \frac{(1 - \beta_k)^3}{\beta_k} \|\nabla F(\mathbf{x}^{k-1}) - \nabla F(\mathbf{x}^k)\|^2 \\ &= (1 - \beta_k) \|\mathbf{v}^{k-1} - \nabla F(\mathbf{x}^{k-1})\|^2 + \beta_k^2 \mathbb{E}[\|\tilde{\nabla}_k - \nabla F(\mathbf{x}^k)\|^2 | \mathcal{F}_k] + \frac{(1 - \beta_k)^2 \|\nabla F(\mathbf{x}^{k-1}) - \nabla F(\mathbf{x}^k)\|^2}{\beta_k} \\ &\leq (1 - \beta_k) \|\mathbf{v}^{k-1} - \nabla F(\mathbf{x}^{k-1})\|^2 + \beta_k^2 \mathbb{E}[\|\tilde{\nabla}_k - \nabla F(\mathbf{x}^k)\|^2 | \mathcal{F}_k] + \frac{\|\nabla F(\mathbf{x}^{k-1}) - \nabla F(\mathbf{x}^k)\|^2}{\beta_k}. \end{aligned}$$

This completes the proof. \blacksquare

Now we are ready to provide the convergence result for our momentum based SBPG.

Theorem 24 *Suppose Assumption 1, 2 and 3 hold. Let $\alpha_k = c\mu\beta_{k+1}$ for any $c \in (0, \frac{1}{2\sqrt{\mu\kappa}}]$. Then*

$$\mathbb{E}[\|\tilde{\mathcal{G}}_{\alpha_r}(\mathbf{x}^r)\|^2] \leq \frac{\Phi^0 - \Phi^* + c\|\mathbf{v}_0 - \nabla F(\mathbf{x}^0)\|^2 + c\sum_{k=1}^N \frac{\beta_k^2 \sigma^2}{m_k}}{\sum_{k=0}^{N-1} \frac{\mu\alpha_k}{8}} = \mathcal{O}\left(\frac{1}{\sum_{k=0}^{N-1} \alpha_k} + \frac{\sum_{k=0}^{N-1} \frac{\alpha_k^2}{m_{k+1}}}{\sum_{k=0}^{N-1} \alpha_k}\right),$$

where r is a random variable with distribution $\mathbb{P}\{r = k\} = \frac{\alpha_k}{\sum_{k=0}^{N-1} \alpha_k}$, for $k = 0, \dots, N-1$.

Proof From Lemma 16 and Cauchy-Young inequality, we have

$$\begin{aligned} \Phi(\mathbf{x}^{k+1}) &\leq \Phi(\mathbf{x}^k) - \frac{1}{\alpha_k} \mathcal{D}_\phi(\mathbf{x}^k, \mathbf{x}^{k+1}) + \frac{\mu}{4\alpha_k} \|\mathbf{x}^k - \mathbf{x}^{k+1}\|^2 + \frac{\alpha_k}{\mu} \|\varepsilon_k\|^2 \\ &\leq \Phi(\mathbf{x}^k) - \frac{1}{2\alpha_k} \mathcal{D}_\phi(\mathbf{x}^k, \mathbf{x}^{k+1}) + \frac{\alpha_k}{\mu} \|\varepsilon_k\|^2. \end{aligned}$$

where we have defined $\boldsymbol{\varepsilon}_k := \nabla F(\mathbf{x}^k) - \mathbf{v}^k$. Summing the above inequality over $k = 0, \dots, N-1$ and rearranging the terms, we get

$$\sum_{k=0}^{N-1} \frac{1}{2\alpha_k} \mathcal{D}_\phi(\mathbf{x}^k, \mathbf{x}^{k+1}) \leq \Phi(\mathbf{x}^0) - \Phi^* + \sum_{k=0}^{N-1} \frac{\alpha_k}{\mu} \|\boldsymbol{\varepsilon}_k\|^2.$$

By applying Lemma 23, we can obtain the following inequality:

$$\beta_k \mathbb{E}[\|\boldsymbol{\varepsilon}_{k-1}\|^2] \leq \mathbb{E}[\|\boldsymbol{\varepsilon}_{k-1}\|^2] - \mathbb{E}[\|\boldsymbol{\varepsilon}_k\|^2] + \beta_k^2 \mathbb{E}[\|\tilde{\nabla}_k - \nabla F(\mathbf{x}^k)\|^2] + \mathbb{E}\left[\frac{\|\nabla F(\mathbf{x}^{k-1}) - \nabla F(\mathbf{x}^k)\|^2}{\beta_k}\right].$$

Hence

$$\sum_{k=0}^{N-1} \beta_{k+1} \mathbb{E}[\|\boldsymbol{\varepsilon}_k\|^2] = \sum_{k=1}^N \beta_k \mathbb{E}[\|\boldsymbol{\varepsilon}_{k-1}\|^2] \leq \|\boldsymbol{\varepsilon}_0\|^2 + \sum_{k=1}^N \beta_k^2 \mathbb{E}[\|\tilde{\nabla}_k - \nabla F(\mathbf{x}^k)\|^2] + \sum_{k=1}^N \mathbb{E}\left[\frac{\|\nabla F(\mathbf{x}^{k-1}) - \nabla F(\mathbf{x}^k)\|^2}{\beta_k}\right].$$

Since $\frac{\alpha_k}{\mu} = c\beta_{k+1}$ for some constant c , we get the following inequality:

$$\sum_{k=0}^{N-1} \frac{1}{2\alpha_k} \mathbb{E}[\mathcal{D}_\phi(\mathbf{x}^k, \mathbf{x}^{k+1})] \leq \Phi(\mathbf{x}^0) - \Phi^* + c \left(\|\boldsymbol{\varepsilon}_0\|^2 + \sum_{k=1}^N \beta_k^2 \mathbb{E}[\|\tilde{\nabla}_k - \nabla F(\mathbf{x}^k)\|^2] + \sum_{k=1}^N \mathbb{E}\left[\frac{\|\nabla F(\mathbf{x}^{k-1}) - \nabla F(\mathbf{x}^k)\|^2}{\beta_k}\right] \right).$$

By using Assumption 3, we obtain that

$$\frac{\|\nabla F(\mathbf{x}^k) - \nabla F(\mathbf{x}^{k+1})\|^2}{\beta_{k+1}} \leq \frac{\kappa}{\beta_{k+1}} \mathcal{D}_\phi(\mathbf{x}^k, \mathbf{x}^{k+1}).$$

Combining above two inequalities, we get

$$\sum_{k=0}^{N-1} \frac{1}{2\alpha_k} \mathbb{E}[\mathcal{D}_\phi(\mathbf{x}^k, \mathbf{x}^{k+1})] \leq \Phi(\mathbf{x}^0) - \Phi^* + c \left(\|\boldsymbol{\varepsilon}_0\|^2 + \sum_{k=1}^N \beta_k^2 \mathbb{E}[\|\tilde{\nabla}_k - \nabla F(\mathbf{x}^k)\|^2] + \sum_{k=0}^{N-1} \frac{\kappa}{\beta_{k+1}} \mathbb{E}[\mathcal{D}_\phi(\mathbf{x}^k, \mathbf{x}^{k+1})] \right).$$

Since $c \leq \frac{1}{2\sqrt{\mu\kappa}}$ and $\frac{\alpha_k}{\mu} = c\beta_{k+1}$, we can deduce that $\frac{c\kappa}{\beta_{k+1}} \leq \frac{1}{4\alpha_k}$. Using this condition, we obtain the inequality:

$$\sum_{k=0}^{N-1} \frac{1}{4\alpha_k} \mathbb{E}[\mathcal{D}_\phi(\mathbf{x}^k, \mathbf{x}^{k+1})] \leq \Phi(\mathbf{x}^0) - \Phi^* + c \left(\|\boldsymbol{\varepsilon}_0\|^2 + \sum_{k=1}^N \beta_k^2 \mathbb{E}[\|\tilde{\nabla}_k - \nabla F(\mathbf{x}^k)\|^2] \right).$$

Note that $\mathcal{D}_\phi(\mathbf{x}^k, \mathbf{x}^{k+1}) \geq \frac{\mu}{2} \|\mathbf{x}^k - \mathbf{x}^{k+1}\|^2 = \frac{\mu\alpha_k^2}{2} \|\tilde{\mathcal{G}}_{\alpha_k}(\mathbf{x}^k)\|^2$ and by the definition of the random variable a , we get

$$\mathbb{E}[\|\tilde{\mathcal{G}}_{\alpha_a}(\mathbf{x}^a)\|^2] \leq \frac{\Phi^0 - \Phi^* + c\|\boldsymbol{\varepsilon}_0\|^2 + c\sum_{k=1}^N \frac{\beta_k^2 \sigma^2}{m_k}}{\sum_{k=0}^{N-1} \frac{\mu\alpha_k}{8}} = \mathcal{O}\left(\frac{1}{\sum_{k=0}^{N-1} \alpha_k} + \frac{\sum_{k=0}^{N-1} \frac{\alpha_k^2}{m_{k+1}}}{\sum_{k=0}^{N-1} \alpha_k}\right),$$

which completes the proof. \blacksquare

Remark 25 Now we give some remarks for Theorem 24.

1. When the sequence $\{\mathbf{x}_k\}$ is bounded, an alternative assumption to Assumption 3 is that $C = \mathbb{R}^d$ and ϕ has a locally Lipschitz gradient, as made in (Bolte et al., 2018, Theorem 4.1) and (Latafat et al., 2022, Theorem 4.7). Under these assumptions, we can conclude that there exists a compact set \mathcal{U} containing $\{\mathbf{x}_k\}$. Therefore, there exists $L_{\phi, \mathcal{U}} > 0$ such that $\nabla\phi$ is Lipschitz continuous over \mathcal{U} , and we can derive that $\|\nabla F(\mathbf{x}) - \nabla F(\mathbf{y})\|^2 \leq L_F^2 L_{\phi, \mathcal{U}}^2 \|\mathbf{x} - \mathbf{y}\|^2 \leq \frac{2L_F^2 L_{\phi, \mathcal{U}}^2}{\mu} \mathcal{D}_\phi(\mathbf{x}, \mathbf{y})$ holds.
2. Compared to the results presented in Theorem 19, it is worth noting that even when keeping m_k constant, we can still achieve convergence to zero error bound by carefully selecting the stepsize sequence $\{\alpha_k\}$. A typical stepsize condition is that $\sum_k \alpha_k = \infty$, $\sum_k \alpha_k^2 < \infty$, which coincides with the classical stepsize condition that guarantees a sufficient but not too fast decrease of the stepsize, as discussed in Bertsekas and Tsitsiklis (2000). Therefore, by incorporating the momentum technique, we can achieve an improved convergence with negligible additional computation costs. This desirable convergence property theoretically supports the use of SBPG with momentum for large-scale problems, such as deep neural networks, without the need to increase the mini-batch size.

4. Application of MSBPG in deep neural networks

In this section, we present a detailed description of MSBPG applied to training deep neural networks. Throughout this section, we assume that the optimization domain \overline{C} is the entire space \mathbb{R}^d , so that $\phi \in \mathcal{M}(\mathbb{R}^d)$ and $F \in \mathcal{C}^1(\mathbb{R}^d)$. For simplicity, we omit the explicit mention of the feasible set \mathbb{R}^d in this section. The optimization problem we consider here is given by:

$$\min_{\mathbf{W}} \underbrace{\frac{1}{N} \sum_{i=1}^N \mathcal{L}(\mathcal{DNN}(\mathbf{W}, \mathbf{x}_i), y_i)}_{F(\mathbf{W})} + \lambda \|\mathbf{W}\|_1, \quad (11)$$

where $\mathcal{DNN}(\mathbf{W}, \mathbf{x})$ is the neural network function with training parameters \mathbf{W} and input data \mathbf{x} , \mathcal{L} is the loss function that measures the difference between the output of the neural network $\mathcal{DNN}(\mathbf{W}, \mathbf{x}_i)$ and the label y_i , $F(\mathbf{W})$ is the training loss evaluated on the training dataset $\{(\mathbf{x}_i, y_i)\}_{i=1}^N$, and $\lambda \|\mathbf{W}\|_1$ is the L_1 regularization term that is often used to avoid overfitting in training deep neural networks (Ng, 2004). To illustrate the neural network function $\mathcal{DNN}(\mathbf{W}, \mathbf{x})$, in the L -layer fully connected neural network, we have $\mathbf{W} = [\mathbf{W}_1, \mathbf{W}_2, \dots, \mathbf{W}_L]$ and

$$\mathcal{DNN}(\mathbf{W}, \mathbf{x}) = \sigma_L(\mathbf{W}_L(\sigma_{L-1}(\mathbf{W}_{L-1}(\dots(\sigma_1(\mathbf{W}_1 \mathbf{x}))\dots))), \quad (12)$$

where σ_i is the nonlinear activation function. In this paper, we focus on smooth activation functions.

At the k -th iteration, MSBPG has the following update scheme:

$$\mathbf{v}_k = (1 - \beta_k) \mathbf{v}^{k-1} + \beta_k \widetilde{\nabla}_k \quad (13)$$

$$\mathbf{W}^{k+1} = \underset{\mathbf{W}}{\operatorname{argmin}} \langle \mathbf{v}^k, \mathbf{W} - \mathbf{W}^k \rangle + \frac{1}{\alpha_k} \mathcal{D}_\phi(\mathbf{W}, \mathbf{W}^k) + \lambda \|\mathbf{W}\|_1, \quad (14)$$

where $\widetilde{\nabla}_k$ is mini-batch gradient computed by automatic differentiation (Griewank and Walther, 2008). Omitting all the constants, the subproblem takes the form of:

$$\mathbf{W}^{k+1} = \underset{\mathbf{W}}{\operatorname{argmin}} \phi(\mathbf{W}) + \langle \mathbf{p}^k, \mathbf{W} \rangle + \alpha_k \lambda \|\mathbf{W}\|_1, \quad (15)$$

where $\mathbf{p}^k = \alpha_k \mathbf{v}^k - \nabla \phi(\mathbf{W}^k)$. Here we adopt the kernel function $\phi(\mathbf{W}) = \frac{1}{2} \|\mathbf{W}\|^2 + \frac{\delta}{r} \|\mathbf{W}\|^r$ ($r \geq 2$) for training neural networks, and then we have an explicit solution for (15) in Proposition 26.

Proposition 26 *Given $\mathbf{p}^k \in \mathbb{R}^d$, positive constant α_k , λ , and the kernel function $\phi(\mathbf{W}) = \frac{1}{2} \|\mathbf{W}\|^2 + \frac{\delta}{r} \|\mathbf{W}\|^r$ ($r \geq 2$, $\delta > 0$). The solution of the subproblem (15) is given by*

$$\mathbf{W}^{k+1} = -t^* \mathbf{p}^+,$$

where t^* is the unique positive real root of the equation

$$(\delta \|\mathbf{p}^+\|^{r-2}) t^{r-1} + t - 1 = 0, \quad (16)$$

and \mathbf{p}^+ is given by

$$\mathbf{p}^+ = \underset{\mathbf{p}}{\operatorname{argmin}} \left\{ \frac{1}{2} \|\mathbf{p} - \mathbf{p}^k\|^2 + \alpha_k \lambda \|\mathbf{p}\|_1 \right\}$$

which has an explicit expression given by $\mathbf{p}_j^+ = \operatorname{sign}(\mathbf{p}_j^k) \max(|\mathbf{p}_j^k| - \alpha_k \lambda, 0)$ for the j -th coordinate.

Proof The optimality condition of (15) is given by

$$0 = \mathbf{W}^{k+1} (1 + \delta \|\mathbf{W}^{k+1}\|^{r-2}) + \mathbf{p}^k + \alpha_k \lambda \mathbf{\Gamma}^k, \text{ where } \mathbf{\Gamma}^k \in \partial \|\cdot\|_1(\mathbf{W}^{k+1}).$$

Let $\mathbf{p}^+ = \mathbf{p}^k + \alpha_k \lambda \mathbf{\Gamma}^k$. By the optimality condition, we have $\mathbf{W}^{k+1} = -t \mathbf{p}^+$ for some positive scalar t , and

$$(-t - \delta \|\mathbf{p}^+\|^{r-2} t^{r-1} + 1) \mathbf{p}^+ = 0.$$

If $\mathbf{p}^+ \neq 0$, then $\delta \|\mathbf{p}^+\|^{r-2} t^{r-1} + t - 1 = 0$. If $\mathbf{p}^+ = 0$, then $\mathbf{W}^{k+1} = -t \mathbf{p}^+ = 0$. Since $t > 0$, then we have $\partial \|\cdot\|_1(\mathbf{W}^{k+1}) = \partial \|\cdot\|_1(-t \mathbf{p}^+) = -\partial \|\cdot\|_1(\mathbf{p}^+)$. Recall the definition of \mathbf{p}^+ , we have

$$\mathbf{p}^+ = \mathbf{p}^k + \alpha_k \lambda \mathbf{\Gamma}^k \in \mathbf{p}^k - \alpha_k \lambda \partial \|\cdot\|_1(\mathbf{p}^+),$$

which is sufficient and necessary optimality condition of the convex optimization problem:

$$\mathbf{p}^+ = \underset{\mathbf{p}}{\operatorname{argmin}} \left\{ \frac{1}{2} \|\mathbf{p} - \mathbf{p}^k\|^2 + \alpha_k \lambda \|\mathbf{p}\|_1 \right\}.$$

This completes the proof by noting the the above minimization problem is the well-known soft threshold operator, see for example Friedman et al. (2010). \blacksquare

Example 1 *In the absence of regularization, that is, when $\lambda = 0$, then $\mathbf{p}^+ = \mathbf{p}^k$ and the update formula for MSBPG at the k -th iteration simplifies to $\mathbf{W}^{k+1} = -t^* \mathbf{p}^k$, where t^* is the positive root of the equation (16). In this case, $\mathbf{W}^{k+1} = t^*(\nabla \phi(\mathbf{W}^k) - \alpha_k \mathbf{v}^k)$.*

Example 2 *If we set the L_1 regularization parameter λ to zero and choose the kernel function simply as the Euclidean distance, i.e. $\delta = 0$, then SBPG reduces to SGD with momentum. Specifically, we have $t^* = 1$ and the update*

$$\mathbf{W}^{k+1} = \mathbf{W}^k - \alpha_k \mathbf{v}^k.$$

Determining degree of kernel function We now turn our attention to selecting the appropriate parameter r for the kernel function. Intuitively, in order to bound the Hessian of the loss function in (11), particularly when the number of layers L in (12) is large, r should also be chosen to be larger, so that $\nabla^2 F \preceq \frac{1}{\alpha} \nabla^2 \phi$ holds globally for some $\alpha > 0$. However, in this case, a significant numerical issue may arise when computing $\|\mathbf{W}\|^{r-2}$. This problem can be avoided if the deep neural network exhibits some special structure such that a moderate r can make $F(\mathbf{W})$ smooth adaptable with respect to $\phi(\mathbf{W})$. For simplicity of analysis, we assume all the given label y_i as zero and consider a sum of squares error loss function. Then, we have a two-layer model defined as follows:

$$\min_{\mathbf{W}=(\mathbf{u},\mathbf{v})} F(\mathbf{W}) = \frac{1}{2} \|\sigma(\text{Mat}(\mathbf{u})(g(\mathbf{v})))\|^2, \quad (17)$$

where $\mathbf{v} \in \mathbb{R}^n$, $\mathbf{u} \in \mathbb{R}^{km}$, $g : \mathbb{R}^n \rightarrow \mathbb{R}^m$, $\sigma : \mathbb{R} \rightarrow \mathbb{R}$, $\text{Mat}(\mathbf{u}) \in \mathbb{R}^{k \times m}$ and $\sigma(\cdot)$ is a coordinate-wise operator. Notably, any deep neural network can be recast as the two-layer model given by (17). For instance, if we define $\mathbf{v} = (\mathbf{W}_1, \dots, \mathbf{W}_{L-1})$, $\mathbf{u} = \text{Vec}(\mathbf{W}_L)$, $g(\mathbf{W}_1, \dots, \mathbf{W}_{L-1}) = \sigma_{L-1}(\mathbf{W}_{L-1}(\dots(\sigma_1(\mathbf{W}_1 \mathbf{x}))\dots))$, then model (12) can be reformulated as (17). We make the following assumptions in this section, which guarantees that we can find a polynomial kernel function ϕ with a moderate degree, such that F in (17) is smooth adaptable to ϕ .

Assumption 4 σ is twice differentiable and σ' and $\sigma \cdot \sigma''$ are globally bounded.

Assumption 5 g is twice differentiable. All partial derivatives of order zero, one, and two of g are globally bounded.

Remark 27 Now we give some remarks on the above assumptions.

1. Assumption 4 is typically valid for various commonly used smooth activation functions. For example, the sigmoid function $\sigma(x) = \frac{1}{1+e^{-x}}$ satisfies global boundedness for both σ and σ'' . Certain activation function may not have bounded function value, such as GELU (Hendrycks and Gimpel, 2016), which takes the formulation of $\sigma(x) = x\Phi(x)$ where Φ is the standard Gaussian cumulative distribution function. Nonetheless, the product $\sigma \cdot \sigma''$ is globally bounded. Another type of activation function satisfying Assumption 4 is the smoothed ReLU function, for example, the following smoothed ReLU function, which we will consider in our numerical experiments:

$$\sigma_\epsilon(x) = \begin{cases} 0 & x \leq 0 \\ x^3 \left(\frac{1}{\epsilon^2} - \frac{x}{2\epsilon^3} \right) & 0 < x \leq \epsilon \\ x - \frac{\epsilon}{2} & x > \epsilon. \end{cases}$$

We observe that as ϵ tends to zero, σ_ϵ converges to the ReLU function. It is straightforward to verify that $\sigma_\epsilon \cdot \sigma_\epsilon''$ is globally bounded. Specifically, $\frac{3}{4}$ is a uniform bound on $\sigma_\epsilon \cdot \sigma_\epsilon''$ for $\epsilon \in (0, \frac{1}{2})$.

2. In many popular neural network frameworks, batch normalization (BN) layers (Ioffe and Szegedy, 2015) are often used before the fully connected layers. For example, in the VGG (Simonyan and Zisserman, 2014) and ResNet (He et al., 2016), BN layers

are usually used before the last linear layer. In this case, we can treat all layers except the last one as one layer, which can be modeled as (17). It is expected that the BN layer can make the function g sufficiently smooth, thereby satisfying Assumption 5.

By applying the chain rule, we can compute the Hessian of F and determine a suitable degree parameter r in the kernel function, which will ensure that $\nabla^2 F$ is bounded by $\nabla^2 \phi$ globally. Consequently, F is smooth adaptable with respect to ϕ . In order to compute the Hessian of F , two formulas are required, which can be verified directly.

Lemma 28 *Let $\mathbf{u} \in \mathbb{R}^{km}$, $\mathbf{g} \in \mathbb{R}^m$, $\mathbf{A} \in \mathbb{R}^{n \times m}$ and $\mathbf{b} \in \mathbb{R}^k$. Consider two linear maps: $\mathbf{u} \mapsto \text{Mat}(\mathbf{u})\mathbf{g}$ and $\mathbf{u} \mapsto \mathbf{A}(\text{Mat}(\mathbf{u}))^T\mathbf{b}$, then, the Jacobian of the two maps are given by*

$$\begin{aligned} J_{\mathbf{u}}[\text{Mat}(\mathbf{u})\mathbf{g}] &= \mathbf{g}^T \otimes \mathbb{I}_k, \\ J_{\mathbf{u}}[\mathbf{A}(\text{Mat}(\mathbf{u}))^T\mathbf{b}] &= \mathbf{A} \otimes \mathbf{b}^T. \end{aligned}$$

Proposition 29 *Suppose Assumptions 4 and 5 hold. Then, for any given $\delta > 0$ and any $r \geq 4$, the function F defined in (17) is smooth adaptable with respect to $\phi(\mathbf{W}) = \frac{1}{2}\|\mathbf{W}\|^2 + \frac{\delta}{r}\|\mathbf{W}\|^r$.*

Proof We denote $\text{Mat}(\mathbf{u})$ by \mathbf{M} . The Jacobian of g is denoted by Jg , while its transpose is denoted by $J^T g$. \mathbb{I}_k is $k \times k$ identity matrix. Using Lemma 28, we can compute the Jacobian and Hessian of F as follows:

Jacobian of F :

$$\begin{aligned} \frac{\partial F}{\partial \mathbf{u}} &= (g(\mathbf{v}) \otimes \mathbb{I}_k) [\sigma'(\mathbf{M}g(\mathbf{v})) \circ \sigma(\mathbf{M}g(\mathbf{v}))], \\ \frac{\partial F}{\partial \mathbf{v}} &= J^T g(\mathbf{v})\mathbf{M}^T [\sigma'(\mathbf{M}g(\mathbf{v})) \circ \sigma(\mathbf{M}g(\mathbf{v}))]. \end{aligned} \tag{18}$$

Hessian of F :

$$\frac{\partial^2 F}{\partial \mathbf{u}^2} = (1) + (2), \tag{19}$$

$$\begin{aligned} \text{where (1)} &= (g(\mathbf{v}) \otimes \mathbb{I}_k) \text{Diag}(\sigma(\mathbf{M}g(\mathbf{v})) \circ \sigma''(\mathbf{M}g(\mathbf{v}))) (\mathbf{g}^T(\mathbf{v}) \otimes \mathbb{I}_k) \\ \text{(2)} &= (g(\mathbf{v}) \otimes \mathbb{I}_k) \text{Diag}(\sigma'(\mathbf{M}g(\mathbf{v})) \circ \sigma'(\mathbf{M}g(\mathbf{v}))) (\mathbf{g}^T(\mathbf{v}) \otimes \mathbb{I}_k). \end{aligned}$$

$$\frac{\partial^2 F}{\partial \mathbf{u} \partial \mathbf{v}} = (1) + (2) + (3),$$

$$\begin{aligned} \text{where (1)} &= (J^T g(\mathbf{v})) \otimes [\sigma'(\mathbf{M}g(\mathbf{v})) \circ \sigma'(\mathbf{M}g(\mathbf{v}))]^T \\ \text{(2)} &= J^T g(\mathbf{v})\mathbf{M}^T \text{Diag}[\sigma(\mathbf{M}g(\mathbf{v})) \circ \sigma''(\mathbf{M}g(\mathbf{v}))] (\mathbf{g}^T(\mathbf{v}) \otimes \mathbb{I}_k) \\ \text{(3)} &= J^T g(\mathbf{v})\mathbf{M}^T \text{Diag}[\sigma'(\mathbf{M}g(\mathbf{v})) \circ \sigma'(\mathbf{M}g(\mathbf{v}))] (\mathbf{g}^T(\mathbf{v}) \otimes \mathbb{I}_k). \end{aligned} \tag{20}$$

$$\frac{\partial^2 F}{\partial \mathbf{v}^2} = (1) + (2) + (3),$$

$$\begin{aligned} \text{where (1)} &= D^2 g(\mathbf{v}) [\mathbf{M}^T [\sigma'(\mathbf{M}g(\mathbf{v})) \circ \sigma(\mathbf{M}g(\mathbf{v}))]] = \sum d_i \nabla^2 g_i(\mathbf{v}) \\ \text{(2)} &= J^T g(\mathbf{v})\mathbf{M}^T \text{Diag}[\sigma(\mathbf{M}g(\mathbf{v})) \circ \sigma''(\mathbf{M}g(\mathbf{v}))] \mathbf{M} J g(\mathbf{v}) \\ \text{(3)} &= J^T g(\mathbf{v})\mathbf{M}^T \text{Diag}[\sigma'(\mathbf{M}g(\mathbf{v})) \circ \sigma'(\mathbf{M}g(\mathbf{v}))] \mathbf{M} J g(\mathbf{v}), \end{aligned} \tag{21}$$

where $\mathbf{d} = \mathbf{M}^T[\sigma'(\mathbf{M}g(\mathbf{v})) \circ \sigma(\mathbf{M}g(\mathbf{v}))]$. Now, we are ready to prove this proposition. For any $\mathbf{w} \in \mathbb{R}^{km+n}$ and $\mathbf{h} = [\mathbf{h}^u; \mathbf{h}^v] \in \mathbb{R}^{km+n}$, it suffices to prove that $\langle \nabla^2 F(\mathbf{w})\mathbf{h}, \mathbf{h} \rangle = \mathcal{O}(\langle \nabla^2 \phi(\mathbf{w})\mathbf{h}, \mathbf{h} \rangle)$. From (19)(20)(21) and Assumption 4, 5, we can easily get $\langle \nabla^2 F(\mathbf{w})\mathbf{h}, \mathbf{h} \rangle = \mathcal{O}((1 + \|\mathbf{w}\|^2)\|\mathbf{h}\|^2)$. On the other hand, $\nabla^2 \phi(\mathbf{w}) = I(1 + \|\mathbf{w}\|^{r-2}) + (r-2)\|\mathbf{w}\|^{r-4}\mathbf{w}\mathbf{w}^T$. Hence $\langle \nabla^2 \phi(\mathbf{w})\mathbf{h}, \mathbf{h} \rangle \geq (1 + \|\mathbf{w}\|^{r-2})\|\mathbf{h}\|^2$. So, we only require $r-2 \geq 2$. This completes the proof. \blacksquare

Layerwise kernel function In Proposition 26, the kernel function $\phi(\mathbf{W}) = \frac{1}{2}\|\mathbf{W}\|^2 + \frac{\delta}{r}\|\mathbf{W}\|^r$ is used, which means we adopt the same Bregman distance for all layers of deep neural networks. However, different layers have different optimization property for deep neural networks (You et al., 2019), and computing $\|\mathbf{W}\|^r$ with $r > 2$ may result in numerical issues for neural networks with millions of parameters, such as in VGG (Simonyan and Zisserman, 2014). To take advantage of the layerwise structure of neural networks, we design a layerwise kernel function for a L -layer neural network as follows:

$$\phi(\mathbf{W}) = \sum_{i=1}^L \phi_i(\mathbf{W}_i), \quad \phi_i(\mathbf{W}_i) = \frac{1}{2}\|\mathbf{W}_i\|^2 + \frac{\delta}{r}\|\mathbf{W}_i\|^r. \quad (22)$$

Note that δ and r can vary from layer to layer, here we take the same δ and r for different layers for simplicity. Then, we have the Bregman distance taking the form $\mathcal{D}_\phi = \sum_{i=1}^L \mathcal{D}_{\phi_i}$. By employing this Bregman distance in subproblem (14), our MSBPG algorithm can be implemented in a layerwise manner. See the details in Algorithm 1.

Algorithm 1 Momentum based Stochastic Bregman Proximal Gradient (MSBPG) for training neural networks

- 1: **Input:** Total number of iterations K , stepsize α_k , momentum parameter β_k , δ and r to determine the kernel function ϕ .
 - 2: **Initialize:** Set $\mathbf{W} = \mathbf{W}^0$, $\mathbf{v}_0 = 0$.
 - 3: **for** $k = 0, \dots, K-1$ **do**
 - 4: Compute mini-batch gradient $\tilde{\nabla}_k$;
 - 5: Compute SMAE: $\mathbf{v}^k = (1 - \beta_k)\mathbf{v}^{k-1} + \beta_k \tilde{\nabla}_k$;
 - 6: **for** $i = 1, \dots, L$ **do**
 - 7: $\mathbf{p}_i^k = \alpha_k \mathbf{v}_i^k - \nabla \phi(\mathbf{W}_i^k)$;
 - 8: $\mathbf{p}_i^+ = \operatorname{argmin}_{\mathbf{p}_i} \{\frac{1}{2}\|\mathbf{p}_i - \mathbf{p}_i^k\|^2 + \alpha_k \lambda \|\mathbf{p}_i\|_1\}$;
 - 9: Solve $(\delta \|\mathbf{p}_i^+\|^{r-2})t_i^{r-1} + t_i - 1 = 0$ to get t_i^k ;
 - 10: $\mathbf{W}_i^{k+1} = -t_i^k \mathbf{p}_i^+$;
 - 11: **end for**
 - 12: **end for**
 - 13: **Output:** $\mathbf{W}^1, \dots, \mathbf{W}^K$.
-

Mitigating gradient explosion In the training of deep neural networks, gradient explosion is a common undesired phenomenon, where the gradients of the loss function grow exponentially from layer to layer, leading to numerical instability or even collapse of the training process (Hochreiter, 1991; Manchev and Spratling, 2020). The reasons for gradient

explosion include selecting a large stepsize and choosing an improper initialization for the model’s parameters (Pascanu et al., 2013). In the following, we will show that MSBPG provides a novel approach to mitigate gradient explosion. Considering MSBPG without regularization, the update rule is given by:

$$\mathbf{W}_i^{k+1} = -t_i^k \mathbf{p}_i^k = t_i^k \left((1 + \delta \|\mathbf{W}_i^k\|^{r-2}) \mathbf{W}_i^k - \alpha_k \mathbf{v}_i^k \right), \quad (23)$$

where $t_i^k \in (0, 1)$ is the unique positive root of

$$\left(\delta \left\| (1 + \delta \|\mathbf{W}_i^k\|^{r-2}) \mathbf{W}_i^k - \alpha_k \mathbf{v}_i^k \right\|^{r-2} \right) t^{r-1} + t - 1 = 0. \quad (24)$$

Combining (23) and (24), we have the following equivalent implicit update scheme for the i -th layer:

$$\mathbf{W}_i^{k+1} = \frac{1 + \delta \|\mathbf{W}_i^k\|^{r-2}}{1 + \delta \|\mathbf{W}_i^{k+1}\|^{r-2}} \mathbf{W}_i^k - \frac{\alpha_k}{1 + \delta \|\mathbf{W}_i^{k+1}\|^{r-2}} \mathbf{v}_i^k. \quad (25)$$

It is observed in practice that with large stepsize or large initial point, the gradient \mathbf{v}_i^k tends to explode if no scaling is done, while the norm of the weight $\|\mathbf{W}_i^{k+1}\|$ also tends to be large. In (25), we see that by scaling the gradient with $\frac{1}{1 + \delta \|\mathbf{W}_i^{k+1}\|^{r-2}}$, the weight \mathbf{W}_i^{k+1} is relieved from moving excessively in the direction of the gradient to avoid rapid growth of its norm. At the same time, we can also see that if the norm $\|\mathbf{W}_i^{k+1}\|$ does not change drastically, the coefficient of \mathbf{W}_i^k in (25) will be maintained to be approximately 1. Thus in (25), we see an automatic scaling of the gradient to avoid rapid growth of the weight and hence also mitigating subsequent gradient explosion.

Experimental results in Section 5.2 indeed verify MSBPG’s ability to mitigate gradient explosion for training deep neural networks. An intuitive illustration of MSBPG’s “pull-back” ability is given in Figure 11 in Appendix B, and this “pull-back” ability originates from the Bregman proximity model and the polynomial kernel function we adopt.

Improving generalization capacity From (25) we can see that MSBPG employs a scaling for the gradient during the update of the parameters as a result of adopting a Bregman proximity model and a polynomial kernel function. This scaling not only helps to mitigate the gradient explosion phenomenon, but also can improve the generalization capacity of MSBPG. To be specific, at the beginning of the training process, the initial weight of each layer \mathbf{W}_i tends to have a larger norm $\|\mathbf{W}_i\|$ and therefore MSBPG takes a cautious update at the beginning phase of training. As the training goes on, due to the effect of regularization, either L_1 or L_2 regularization, the norm of each layer’s weight $\|\mathbf{W}_i\|$ becomes smaller, and MSBPG can then take bolder update of the parameters. This implicit training strategy of MSBPG is in agreement with the idea of a heuristic deep learning training technique called “learning rate warm-up” (Gotmare et al., 2018), which benefits the training stability and generalization performance (Liu et al., 2019). Experimental results in Section 5.2 also testify the excellent generalization capacity of MSBPG.

5. Numerical experiments

In this section, we conduct numerical experiments to showcase the effectiveness and robustness of MSBPG in comparison to modern solvers commonly used in deep learning. We

assess the impact of stepsize and initial point selection on the performance of our method. Our experiments consist of two parts. In the first part, we use a quadratic inverse problem as a toy example to illustrate the capabilities of vanilla SBPG. The second part is the main focus of this section, where we evaluate the performance of MSBPG in training deep neural networks. The experiments for the quadratic inverse problem are conducted using MATLAB R2021b on a Windows workstation equipped with a 12-core Intel Xeon E5-2680 @ 2.50GHz processor and 128GB of RAM. For the deep learning experiments, we conducted the experiments using PyTorch running on a single RTX3090 GPU.

5.1 Quadratic inverse problem

The quadratic inverse problem, as formulated in Bolte et al. (2018), is given by:

$$\min \left\{ \Phi(\mathbf{x}) := \frac{1}{4} \underbrace{\sum_{i=1}^n (\langle A_i \mathbf{x}, \mathbf{x} \rangle - b_i)^2}_{F(\mathbf{x})} + \lambda R(\mathbf{x}) : \mathbf{x} \in \mathbb{R}^d \right\},$$

which has practical applications (Beck and Eldar, 2013) that includes the phase retrieval problem as a special case (Luke, 2017). In this experiment, we consider the L_1 regularization $R(\mathbf{x}) = \|\mathbf{x}\|_1$ with $\lambda = 1 \times 10^{-3}$, and solve the quadratic inverse problem using SBPG and stochastic (Euclidean) proximal gradient (SPG) method (Bertsekas, 2011). Notably, SPG is a special case of SBPG, in which $\phi(\mathbf{x}) = \frac{1}{2}\|\mathbf{x}\|^2$. Since the smooth term in the objective function $F(\mathbf{x})$ does not admit a globally Lipschitz continuous gradient, we employ the kernel function $\phi(\mathbf{x}) = \frac{1}{2}\|\mathbf{x}\|^2 + \frac{1}{r}\|\mathbf{x}\|^r$ with $r = 4$. It has been shown in Lu et al. (2018) that any $r \geq 4$ guarantees that F is ϕ -smooth adaptable globally. Moreover, according to Bolte et al. (2018), the smooth adaptable constant L_F can be chosen such that $L_F \geq \sum_{i=1}^n (3\|A_i\|^2 + \|A_i\|\|b_i\|)$ for $r = 4$. In this experiment, we randomly generate the data by the following MATLAB commands:

```
ai = randn(d, 1); Ai = ai * ai';
x_true = sprandn(d, 1, density_x); b_i = x_true' * (Ai * x_true);
```

The true solution for the quadratic inverse problem is chosen as a sparse vector \mathbf{x}^* that satisfies $\langle A_i \mathbf{x}^*, \mathbf{x}^* \rangle = b_i$ for $i = 1, \dots, n$. We set the mini-batch size for all algorithms to be $m = 1$. To evaluate the effectiveness of each algorithm, we use the following criterion that takes into account the possibility of critical points being local minimum or saddle points:

$$\epsilon_k = \max \left\{ \|\mathcal{G}(\mathbf{x}^k)\|, \epsilon_{\text{obj}} := \frac{\text{obj}_k - \text{obj}_*}{1 + \text{obj}_*} \right\},$$

where $\text{obj}_k = \Phi(\mathbf{x}^k)$ and $\text{obj}_* = \Phi(\mathbf{x}^*)$. The term $\|\mathcal{G}(\mathbf{x}^k)\|$ measures the stationarity of the solution, while a small ϵ_{obj} indicates that the solution is a "nearly" global minimum.

We conduct experiments on a problem with data size $d = 100$ and `density_x = 0.05`. All methods are run until they reach an accuracy of $\epsilon_k \leq 0.01$ within a time limit of 30 seconds. To ensure statistical significance, we run each algorithm 10 times and report the

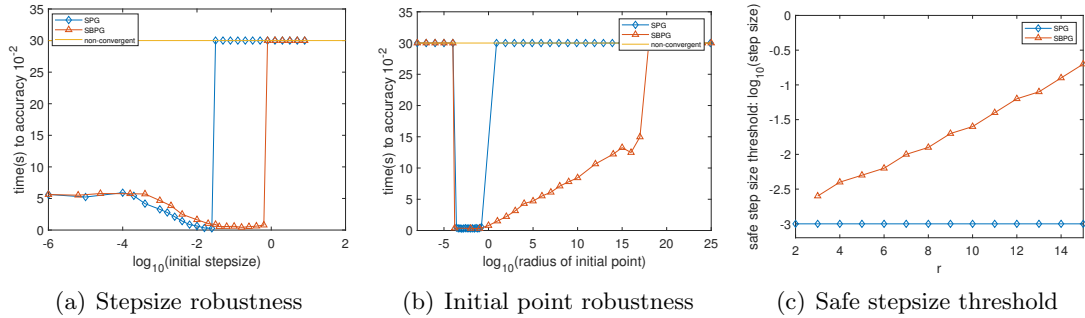


Figure 2: Comparison of SBPG and SPG in terms of their robustness with respect to stepsize and initial point selection. A method is considered non-convergent if it fails to reach an accuracy of $\epsilon_k < 10^{-2}$ within 30 seconds or if it collapses. Generally, choosing large stepsize and large radius for the initial point can cause an algorithm to collapse. The safe stepsize threshold is the maximum stepsize (constant schedule) that a method does not collapse. We run 10 tests for each algorithm and report the median of the results.

median value. The results are presented in Figure 2. For Figures 2(a), we randomly select initial points within a ball centered at the origin with radius 1×10^{-2} . We use the stepsize schedule of $\alpha_k = \max \left\{ 10^{-4}, \frac{\alpha_0}{\sqrt{1+k}} \right\}$, where α_0 is the initial stepsize. For Figure 2(b), we set constant stepsize schedule 1×10^{-3} . For Figures 2(c), we randomly select initial points within a ball centered at the origin with radius 1×10^{-2} . We use constant stepsize schedule. To prevent excessively small stepsizes that can slow down all methods, we set a lower bound for the stepsize.

Figure 2(a) demonstrates that SBPG has a larger range of convergent stepsizes than SPG, indicating that SBPG is more robust in terms of stepsize selection. The impact of the initial stepsize on the performance of the algorithms is reported in this figure. Figure 2(b) shows that SBPG is much more robust than SPG in terms of initial point selection. Specifically, SBPG exhibits high resilience to initial point selection and avoids causing the training to collapse. Figure 2(c) reveals that a larger degree r in the kernel function increases the safe stepsize threshold. These observations are partly explained in Section 4. Since a large stepsize and a large radius of the initial point tend to lead to gradient explosion, Bregman proximal mapping helps to pull back the iterate and guide it towards a better solution.

5.2 Deep neural network

For the evaluation of MSBPG’s performance on training deep neural networks, we consider the model with L_2 regularization here for its better generalization capacity:

$$\min_{\mathbf{W}} \underbrace{\frac{1}{N} \sum_{i=1}^N \mathcal{L}(\mathcal{DNN}(\mathbf{W}, \mathbf{x}_i), y_i)}_{F(\mathbf{W})} + \lambda \|\mathbf{W}\|_2^2. \quad (26)$$

We employ MSBPG to solve this large-scale problem. Following AdamW (Loshchilov and Hutter, 2017), we also conduct decoupled weight decay at the end of each iteration for L_2 regularization and do not consider the L_2 regularization term when solving the subproblems. The detailed algorithm is summarized in Algorithm 2. At iteration k , MSBPG first uses automatic differentiation to compute the mini-batch gradient $\tilde{\nabla}_k$. Then, it maintains a bias-corrected gradient estimator $\tilde{\mathbf{v}}^k$ (Kingma and Ba, 2014) and use it to calculate the layerwise \mathbf{p}_i^k . With \mathbf{p}_i^k , MSBPG solves a univariate equation to get t_i^k and update the weight of the i -th layer to \mathbf{W}_i^k . In the end, MSBPG conducts decoupled weight decay as L_2 regularization.

Algorithm 2 MSBPG with L_2 regularization

- 1: **Input:** Total number of training epochs K , momentum coefficient β , stepsize α_k , weight decay coefficient γ , δ and r to determine the kernel function ϕ .
 - 2: **Initialize:** Set $\mathbf{W} = \mathbf{W}^0$, $\mathbf{v}^0 = \mathbf{0}$.
 - 3: **for** $k = 1, \dots, K$ **do**
 - 4: Compute mini-batch gradient $\tilde{\nabla}^k$;
 - 5: $\mathbf{v}^k = \beta \mathbf{v}^{k-1} + (1 - \beta) \tilde{\nabla}^k$, $\tilde{\mathbf{v}}^k = \mathbf{v}^k / (1 - \beta^k)$;
 - 6: **for** $i = 1, \dots, L$ **do**
 - 7: $\mathbf{p}_i^k = \alpha_k \tilde{\mathbf{v}}_i^k - \nabla \phi(\mathbf{W}_i^{k-1})$;
 - 8: Solve $(\delta \|\mathbf{p}_i^k\|^{r-2}) t_i^{r-1} + t_i - 1 = 0$ to get t_i^k ;
 - 9: $\tilde{\mathbf{W}}_i^k = -t_i^k \mathbf{p}_i^k$;
 - 10: **end for**
 - 11: $\mathbf{W}^k = \tilde{\mathbf{W}}^k - \alpha_k \gamma \mathbf{W}^{k-1}$;
 - 12: **end for**
 - 13: **Output:** $\mathbf{W}^1, \dots, \mathbf{W}^K$
-

We conducted extensive experiments on several representative benchmarks, including VGG16 (Simonyan and Zisserman, 2014), ResNet34 (He et al., 2016) on CIFAR10 dataset (Krizhevsky et al., 2009), ResNet34 (He et al., 2016), DenseNet121 (Huang et al., 2017) on CIFAR100 dataset (Krizhevsky et al., 2009), and LSTMs (Hochreiter and Schmidhuber, 1997) on the Penn Treebank dataset (Marcinkiewicz, 1994). We compare MSBPG with the most popular optimization algorithms used for training neural networks, including SGD (Sutskever et al., 2013), Adam (Kingma and Ba, 2014), and AdamW (Loshchilov and Hutter, 2017). Experimental results show that MSBPG has excellent convergence performance and best generalization capacity for both the task that SGD dominates (image classification with CNNs) and the task that Adam dominates (language modeling with LSTMs).

We also conducted experiments to compare MSBPG with SGD on different initial stepsizes and different scales of initial point. Our experimental results demonstrate the robustness of MSBPG in training neural networks.

Before getting into the details of our experiments, we first make a clarification about the activation function. The frequently used activation function ReLU in VGG, ResNet, and DenseNet takes the form of $\text{ReLU}(x) = \max(0, x)$, which is not continuously differentiable. Here we design a smoothing approximation of ReLU with coefficient ϵ , which is twice continuously differentiable and satisfies our Assumption 4, namely,

$$\sigma_\epsilon(x) = \begin{cases} 0 & x \leq 0 \\ x^3 \left(\frac{1}{\epsilon^2} - \frac{x}{2\epsilon^3} \right) & 0 < x \leq \epsilon \\ x - \frac{\epsilon}{2} & x > \epsilon. \end{cases}$$

This activation function has gradient taking the form:

$$\sigma'_\epsilon(x) = \begin{cases} 0 & x \leq 0 \\ x^2 \left(\frac{3}{\epsilon^2} - \frac{2x}{\epsilon^3} \right) & 0 < x \leq \epsilon \\ 1 & x > \epsilon. \end{cases}$$

Note that as ϵ tends to 0, this twice continuously differentiable activation function tends to the ReLU function. We conducted experiments with VGG16 on the CIFAR10 dataset, where we replace all the activation functions in VGG16 by σ_ϵ defined above. As shown in Figure 4, our algorithm MSBPG’s performance does not degrade as ϵ tends to 0. Therefore, in the subsequent experiments, we use the original neural network architectures with the ReLU activation function to evaluate our method MSBPG.

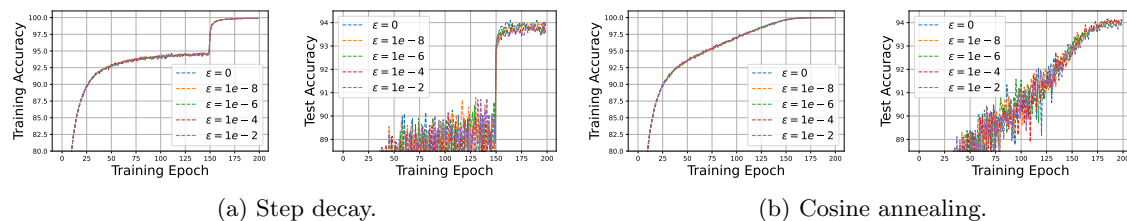


Figure 3: Training and test accuracy (%) of VGG16 on CIFAR10 dataset under two frequently used training settings. Here the activation function of VGG16 adopts smoothed ReLU activation function σ_ϵ with different choices of ϵ ($\epsilon = 0$ denotes adopting the original ReLU activation function).

CNNs on image classification We experimented with VGG16, ResNet34 on the CIFAR10 dataset, and ResNet34, DenseNet121 on CIFAR100 dataset. SGD usually has better generalization performance than adaptive gradient algorithms such as Adam and AdamW when training CNNs on image classification tasks and therefore is the default optimizer in these scenarios (He et al., 2016; Zhou et al., 2020). We used two dominant experimental settings for training neural networks, including reducing the stepsize to 0.1 times its original value near the end of training (Zhuang et al., 2020; Chen et al., 2021; Luo et al., 2019)

and adopting a cosine annealing schedule for the stepsizes (Loshchilov and Hutter, 2016, 2017). The purpose of these two training strategies is to accelerate the convergence of the optimization algorithms so as to give a fair comparison of their generalization capacity. We use the default training hyperparameters of SGD, Adam, and AdamW in these settings (He et al., 2016; Zhuang et al., 2020; Chen et al., 2021), and set MSBPG’s learning rate (initial stepsize) as 0.1, momentum coefficient β as 0.9, weight decay coefficient γ as 1×10^{-3} . For the layerwise kernel function $\phi_i(\mathbf{W}_i) = \frac{1}{2}\|\mathbf{W}_i\|^2 + \frac{\delta}{r}\|\mathbf{W}_i\|^r$, we set $r = 4$, $\delta = 1 \times 10^{-2}$ for VGG16 and $r = 6$, $\delta = 1 \times 10^{-3}$ for ResNet34 on CIFAR10 dataset, and $r = 4$, $\delta = 1 \times 10^{-2}$ for ResNet34 and $r = 4$, $\delta = 1 \times 10^{-3}$ for DenseNet121 on CIFAR100 dataset. From the experimental results in Figure 4, 6, 5, 7, we can see that MSBPG attains 100% training accuracy in all the training settings, unlike Adam which fails to fully converge with the training strategy of reducing the learning rate to 0.1 times of original value at the 150th epoch. Furthermore, MSBPG consistently achieves the best generalization performance for all experimental settings, and attains at least 0.5% test accuracy improvement compared with the second best optimization algorithm. This generalization advantage of MSBPG can be attributed to the Bregman proximity model we adopt.

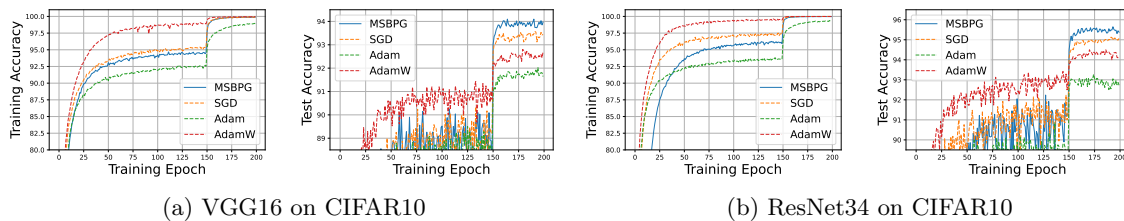


Figure 4: Training and test accuracy (%) of CNNs on CIFAR10 dataset with learning rate reduced to 0.1 times of the original value at the 150th epoch.

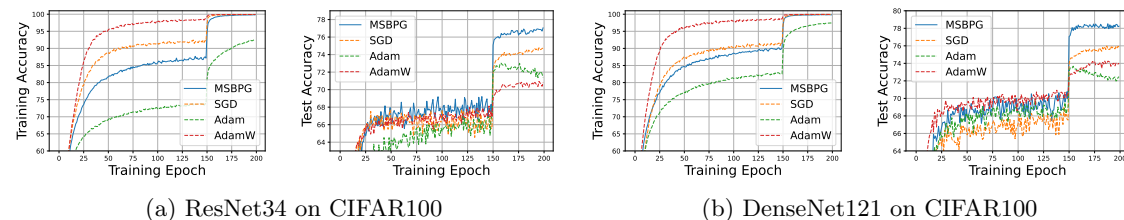


Figure 5: Training and test accuracy (%) of CNNs on CIFAR100 dataset with learning rate reduced to 0.1 times of the original value at the 150th epoch.

LSTMs on language modeling To further evaluate the performance of MSBPG, we conducted experiments on LSTM with the Penn Treebank dataset, and report the training and test perplexity (lower is better). Adam generally have better generalization capacity than SGD on language modeling (Fu et al., 2016; Siami-Namini et al., 2019), and therefore

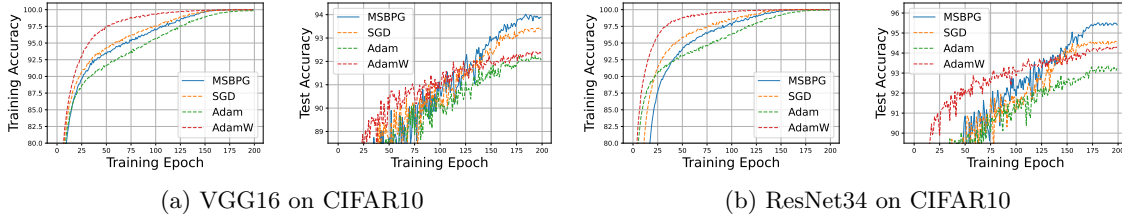


Figure 6: Training and test accuracy (%) of CNNs on CIFAR10 dataset with learning rate using the cosine annealing schedule.

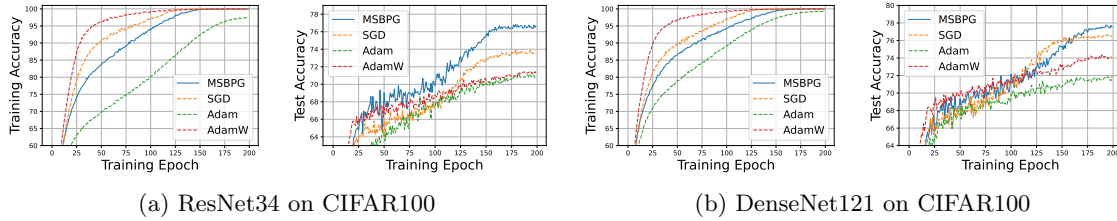


Figure 7: Training and test accuracy (%) of CNNs on CIFAR100 dataset with learning rate using the cosine annealing schedule.

is the default optimization algorithm for training LSTMs. Here we follow the commonly used experimental setting for training LSTMs (Zhuang et al., 2020; Chen et al., 2021), which reduces the stepsize to 0.1 times its original value two times (at 75th epoch and 150th epoch) during the training process. We also conducted experiments with the cosine annealing learning rate (stepsize) schedule (Loshchilov and Hutter, 2016), which is the most frequently used learning rate schedule in practice. For training hyperparameters, we use the default settings for SGD, Adam, and AdamW in training 1-, 2-, 3-layer LSTMs (Zhuang et al., 2020; Chen et al., 2021). For MSBPG, we set its learning rate as 25, 80, 80 for 1-, 2-, 3-layer LSTMs with momentum coefficient $\beta = 0.9$, weight decay coefficient $\gamma = 2 \times 10^{-6}$. For the layerwise kernel function $\phi_i(\mathbf{W}_i) = \frac{1}{2} \|\mathbf{W}_i\|^2 + \frac{\delta}{r} \|\mathbf{W}_i\|^r$, we set $r = 4$ and $\delta = 1 \times 10^{-6}$. From Figure 8 and Figure 9 we can see that MSBPG converges well on training dataset for 1-, 2-, 3-layer LSTMs with both two training strategies. On the other hand, SGD with the cosine annealing learning rate schedule fails to get fully converged on the training dataset as shown in Figure 9. Moreover, MSBPG consistently achieves the best generalization performance for all the experiments with at least 1 unit of test perplexity lower. This excellent generalization capacity again can be attributed to the Bregman proximity model we employ.

Robustness to initial point scale and stepsize As demonstrated in Section 4, MSBPG can mitigate the problem of gradient explosion. Generally, choosing large stepsize and large initial point scale will lead to gradient explosion. Here we conduct experiments with VGG16 on CIFAR10 to verify MSBPG’s robustness in training neural networks. To be specific,

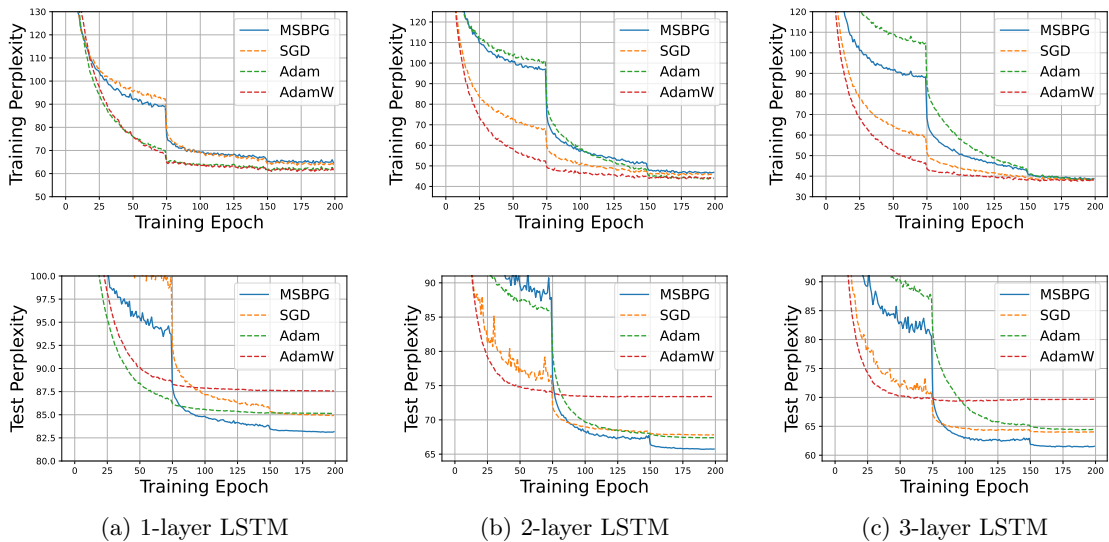


Figure 8: Training and test perplexity (lower is better) of LSTMs on Penn Treebank dataset with learning rate reduced to 0.1 times of the original value at the 75th epoch and 150th epoch.

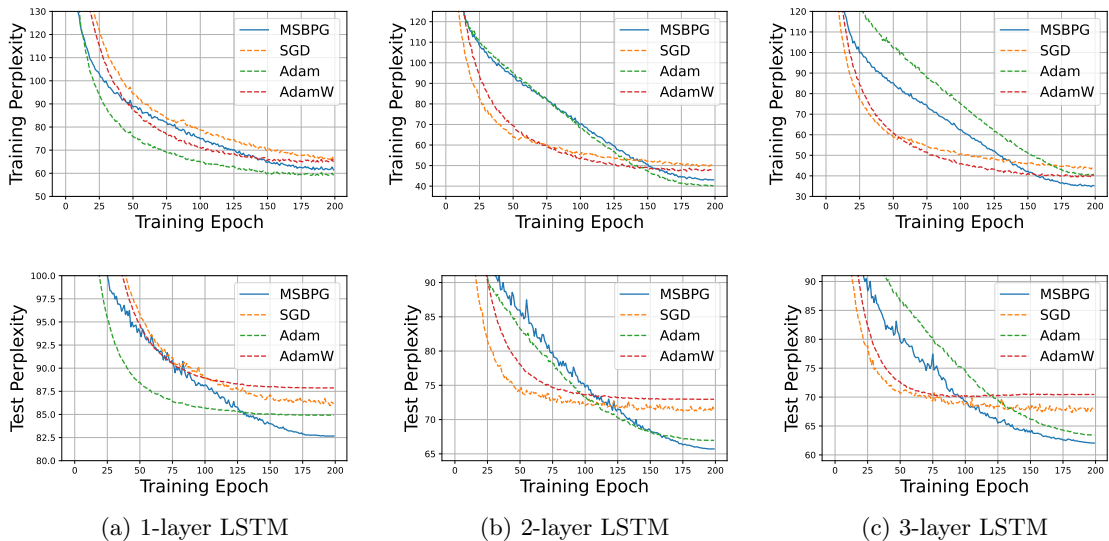


Figure 9: Training and test perplexity (lower is better) of LSTMs on Penn Treebank dataset with learning rate using the cosine annealing schedule.

we compare the performance of MSBPG and SGD with different scales of initial point and different stepsizes, since MSBPG and SGD have the same default learning rate (1×10^{-1}). Adaptive gradient algorithms, on the other hand, have different scale of default learning rate

(1×10^{-3}) and therefore we don't include them in our comparison here. For different choices of initial point scale and stepsize, we run the optimization algorithm for 50 iterations and report the best test accuracy. As we can see from Figure 10, MSBPG is more robust than SGD to large initial points and large stepsizes. Training deep neural networks, which has millions or billions of parameters, is sensitive to the scale of the initial point and stepsize choice. It can be seen from Figure 10 that SGD fails to converge with a slight increase of the initial point scale to 4.6 or increase the stepsize from 0.1 to 0.6. MSBPG, on the other hand, can converge with the initial point scale as large as 20 and stepsize as large as 5. This robustness of MSBPG can ease the tuning of hyperparameters for training neural networks, and can also make the training process more robust to noises and errors.

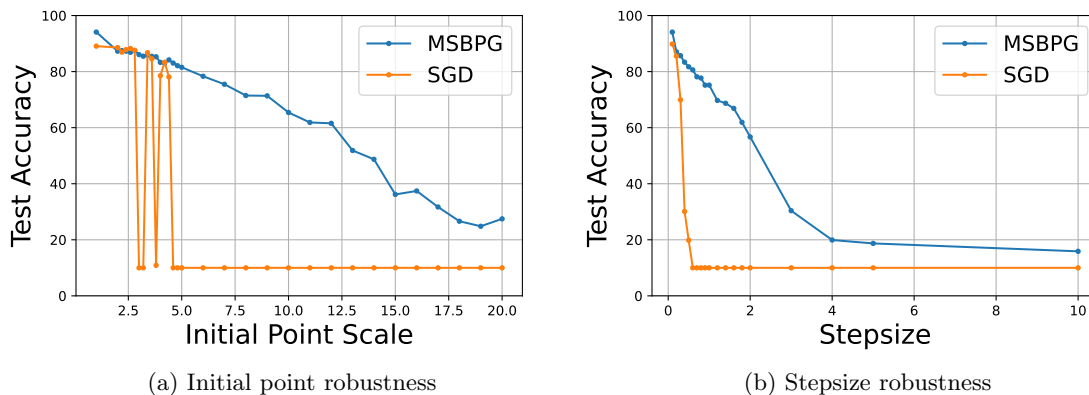


Figure 10: Test accuracy (%) of VGG16 on CIFAR10 dataset with different initial point scale and stepsize choice.

6. Conclusion

In this paper, we consider the problem of minimizing nonconvex composite objectives where the differentiable part does not satisfy Lipschitz smoothness, which is a fundamental assumption made by classical stochastic gradient methods. To overcome this limitation, we investigate a family of stochastic Bregman proximal gradient (SBPG) methods that only require smooth adaptivity of the differentiable part. From a modeling perspective, SBPG replaces the upper quadratic approximation used in SGD with the Bregman proximity measure, which captures the non-Lipschitz geometry and results in a better approximation model. We first formulate the vanilla SBPG and establish its convergence properties under the nonconvex setting without a finite sum structure. We then propose a momentum-based version of SBPG (MSBPG) that further improves its convergence properties, making it well-suited for large-scale applications. To demonstrate the effectiveness of MSBPG, we apply it to train deep neural networks with a polynomial kernel function that ensures the smooth adaptivity of the loss function. We also demonstrate the ability of MSBPG to alleviate gradient explosion during the training of deep neural networks. We conduct numerical experiments on quadratic inverse problems and training deep neural networks to validate

the effectiveness of SBPG. The experimental results on sparse quadratic inverse problems show that SBPG is more robust than classical stochastic (proximal) gradient methods in terms of stepsize selection and initial point selection. Additionally, the experimental results on deep neural networks show that MSBPG outperforms state-of-the-art optimizers in terms of efficiency, robustness of stepsize selection, and yet achieves better generalization performance. In conclusion, our work demonstrates that MSBPG can constitute a valuable addition to the existing family of optimization methods for solving stochastic nonconvex optimization problems. The enhanced robustness, improved convergence results, the ability to alleviate gradient explosion, and negligible extra computational cost thus make MSBPG a promising approach for a broad range of machine learning applications and beyond.

Appendix A. Proofs in Preliminaries

Proof of Lemma 8 First, we prove the uniqueness of the solution. Problem (4) is equivalent to the following problem:

$$\arg \min_{\mathbf{u} \in \bar{C}} \Psi(\mathbf{u}) := \alpha R(\mathbf{u}) + \phi(\mathbf{u}) - \langle \nabla \phi(\mathbf{x}), \mathbf{u} \rangle.$$

We have that

$$\Psi(\mathbf{u}) \geq \alpha R(\mathbf{u}) + \phi(\mathbf{u}) - \|\nabla \phi(\mathbf{x})\| \|\mathbf{u}\| \geq \|\mathbf{u}\| \left(\frac{\alpha R(\mathbf{u}) + \phi(\mathbf{u})}{\|\mathbf{u}\|} - \|\nabla \phi(\mathbf{x})\| \right).$$

As $\|\mathbf{u}\| \rightarrow \infty$, we have $\Psi(\mathbf{u}) \geq \|\mathbf{u}\| \left(\frac{\alpha R(\mathbf{u}) + \phi(\mathbf{u})}{\|\mathbf{u}\|} - \|\nabla \phi(\mathbf{x})\| \right) = \infty$, where we use the fact that ϕ is supercoercive and R is convex. Since Ψ is a proper lower-semicontinuous convex function, by the modern form of Weierstrass theorem (Rockafellar, 1997, Chapter 1), we know that the solution set of (4) is a nonempty compact set. Also note that Ψ is a strictly convex function, which implies the uniqueness of the solution. For any Legendre function ϕ , from (Rockafellar, 1997, Chapter 26), we have $\text{dom } \partial \phi = \text{int } \text{dom } \phi$ with $\partial \phi(\mathbf{x}) = \{\nabla \phi(\mathbf{x})\}$ for all $\mathbf{x} \in \text{int } \text{dom } \phi$. The optimality condition implies that $\partial \phi(\text{Prox}_{\alpha R}^{\phi}(\mathbf{x}))$ is nonempty, which automatically forces $\text{Prox}_{\alpha R}^{\phi}(\mathbf{x}) \in \text{int } \text{dom } \phi$. This completes the proof. \square

Proof of Proposition 12 Note that $\|\nabla \phi(\mathbf{x}^+) - \nabla \phi(\mathbf{x})\| \leq L_{\phi} \|\mathbf{x}^+ - \mathbf{x}\|$ and $\|\nabla F(\mathbf{x}^+) - \nabla F(\mathbf{x})\| \leq L_F L_{\phi} \|\mathbf{x}^+ - \mathbf{x}\|$. By the definition of \mathbf{x}^+ , we have

$$\nabla F(\mathbf{x}^+) - \nabla F(\mathbf{x}) + \frac{\nabla \phi(\mathbf{x}) - \nabla \phi(\mathbf{x}^+)}{\alpha} \in \nabla F(\mathbf{x}^+) + \partial R(\mathbf{x}^+).$$

Thus, we obtain

$$\text{dist}(0, \partial \Phi(\mathbf{x}^+)) \leq \left\| \nabla F(\mathbf{x}^+) - \nabla F(\mathbf{x}) + \frac{\nabla \phi(\mathbf{x}) - \nabla \phi(\mathbf{x}^+)}{\alpha} \right\| \leq \left(L_F L_{\phi} + \frac{L_{\phi}}{\alpha} \right) \|\mathbf{x}^+ - \mathbf{x}\|.$$

Note that $\|\mathbf{x}^+ - \mathbf{x}\| = \alpha \|\mathcal{G}_{\alpha}(\mathbf{x})\|$, which completes the proof. \square

Proof of Proposition 9 By the definition of $\text{Prox}_R^{\phi}(\cdot)$, $x_i \in \partial R(\mathbf{x}_i^+) + \nabla \phi(\mathbf{x}_i^+)$, $i = 1, 2$. Since $\partial R(\cdot)$ is monotone, then $\langle \mathbf{x}_1 - \mathbf{x}_2 - (\nabla \phi(\mathbf{x}_1^+) - \nabla \phi(\mathbf{x}_2^+)), \mathbf{x}_1^+ - \mathbf{x}_2^+ \rangle \geq 0$. From the μ -strong convexity of ϕ , it follows that $\langle \mathbf{x}_1 - \mathbf{x}_2, \mathbf{x}_1^+ - \mathbf{x}_2^+ \rangle \geq \langle \nabla \phi(\mathbf{x}_1^+) - \nabla \phi(\mathbf{x}_2^+), \mathbf{x}_1^+ - \mathbf{x}_2^+ \rangle \geq \mu \|\mathbf{x}_1^+ - \mathbf{x}_2^+\|^2$. Therefore, $\|\mathbf{x}_1^+ - \mathbf{x}_2^+\| \leq \frac{1}{\mu} \|\mathbf{x}_1 - \mathbf{x}_2\|$. \square

Appendix B. Additional Figures

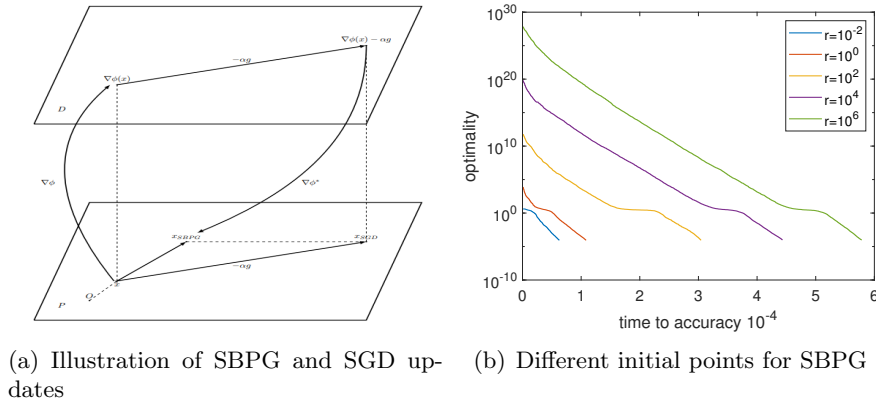


Figure 11: Figure (a) depicts SGD and SBPG updates. SBPG includes a "pull back" mechanism that prevents the point from moving excessively in any given direction. "P" and "D" refer to the primal and dual spaces, respectively, and these terms are commonly used in the mirror descent method literature (see, e.g., Bubeck et al. (2015); Nemirovskij and Yudin (1983)). Figure (b) illustrates the effect of choosing the initial point from a ball of radius r on the SBPG when r changes for the QIP example with $d = 100$ and $n = 5000$. All initial step sizes are set to 1×10^{-3} . As shown in Figure (b), even for an initial point that is far from the optimal point, SBPG can pull back the iterates to the optimal point.

References

- Zeyuan Allen-Zhu. Katyusha: The first direct acceleration of stochastic gradient methods. *Journal of Machine Learning Research*, 18(221):1–51, 2018.
- Heinz H Bauschke, Jérôme Bolte, and Marc Teboulle. A descent lemma beyond Lipschitz gradient continuity: first-order methods revisited and applications. *Mathematics of Operations Research*, 42(2):330–348, 2017.
- Amir Beck and Yonina C Eldar. Sparsity constrained nonlinear optimization: Optimality conditions and algorithms. *SIAM Journal on Optimization*, 23(3):1480–1509, 2013.
- Dimitri P Bertsekas. Incremental proximal methods for large scale convex optimization. *Mathematical Programming*, 129(2):163–195, 2011.
- Dimitri P Bertsekas and John N Tsitsiklis. Gradient convergence in gradient methods with errors. *SIAM Journal on Optimization*, 10(3):627–642, 2000.
- Pascal Bianchi. Ergodic convergence of a stochastic proximal point algorithm. *SIAM Journal on Optimization*, 26(4):2235–2260, 2016.

- Jérôme Bolte, Shoham Sabach, Marc Teboulle, and Yakov Vaisbourd. First order methods beyond convexity and Lipschitz gradient continuity with applications to quadratic inverse problems. *SIAM Journal on Optimization*, 28(3):2131–2151, 2018.
- Lev M Bregman. The relaxation method of finding the common point of convex sets and its application to the solution of problems in convex programming. *USSR Computational Mathematics and Mathematical Physics*, 7(3):200–217, 1967.
- Sébastien Bubeck et al. Convex optimization: Algorithms and complexity. *Foundations and Trends in Machine Learning*, 8(3-4):231–357, 2015.
- Gong Chen and Marc Teboulle. Convergence analysis of a proximal-like minimization algorithm using bregman functions. *SIAM Journal on Optimization*, 3(3):538–543, 1993.
- Jinghui Chen, Dongruo Zhou, Yiqi Tang, Ziyang Yang, Yuan Cao, and Quanquan Gu. Closing the generalization gap of adaptive gradient methods in training deep neural networks. In *Proceedings of the Twenty-Ninth International Conference on International Joint Conferences on Artificial Intelligence*, pages 3267–3275, 2021.
- Aaron Defazio and Léon Bottou. On the ineffectiveness of variance reduced optimization for deep learning. *Advances in Neural Information Processing Systems*, 32, 2019.
- Radu-Alexandru Dragomir, Alexandre d’Aspremont, and Jérôme Bolte. Quartic first-order methods for low-rank minimization. *Journal of Optimization Theory and Applications*, 189:341–363, 2021a.
- Radu Alexandru Dragomir, Mathieu Even, and Hadrien Hendrikx. Fast stochastic bregman gradient methods: Sharp analysis and variance reduction. In *International Conference on Machine Learning*, pages 2815–2825. PMLR, 2021b.
- John Duchi and Yoram Singer. Efficient online and batch learning using forward backward splitting. *Journal of Machine Learning Research*, 10:2899–2934, 2009.
- John Duchi, Elad Hazan, and Yoram Singer. Adaptive subgradient methods for online learning and stochastic optimization. *Journal of Machine Learning Research*, 12(7), 2011.
- J. Friedman, T. Hastie, and R. Tibshirani. Regularization paths for generalized linear models via coordinate descent. *Journal of Statistical Software*, 33(1):1–22, 2010.
- Rui Fu, Zuo Zhang, and Li Li. Using LSTM and GRU neural network methods for traffic flow prediction. In *2016 31st Youth Academic Annual Conference of Chinese Association of Automation (YAC)*, pages 324–328. IEEE, 2016.
- Saeed Ghadimi, Guanghui Lan, and Hongchao Zhang. Mini-batch stochastic approximation methods for nonconvex stochastic composite optimization. *Mathematical Programming*, 155(1-2):267–305, 2016.
- Akhilesh Gotmare, Nitish Shirish Keskar, Caiming Xiong, and Richard Socher. A closer look at deep learning heuristics: Learning rate restarts, warmup and distillation. *arXiv preprint arXiv:1810.13243*, 2018.

- Andreas Griewank and Andrea Walther. *Evaluating derivatives: principles and techniques of algorithmic differentiation*. SIAM, 2008.
- Bin Gu, Wenhan Xian, Zhouyuan Huo, Cheng Deng, and Heng Huang. A unified q-memorization framework for asynchronous stochastic optimization. *The Journal of Machine Learning Research*, 21(1):7761–7813, 2020.
- Filip Hanzely and Peter Richtárik. Fastest rates for stochastic mirror descent methods. *Computational Optimization and Applications*, 79:717–766, 2021.
- Trevor Hastie, Robert Tibshirani, Jerome H Friedman, and Jerome H Friedman. *The elements of statistical learning: data mining, inference, and prediction*, volume 2. Springer, 2009.
- Kaiming He, Xiangyu Zhang, Shaoqing Ren, and Jian Sun. Deep residual learning for image recognition. In *Proceedings of the IEEE conference on Computer Vision and Pattern Recognition*, pages 770–778, 2016.
- Dan Hendrycks and Kevin Gimpel. Gaussian error linear units (gelus). *arXiv preprint arXiv:1606.08415*, 2016.
- Jean-Baptiste Hiriart-Urruty and Claude Lemaréchal. *Convex analysis and minimization algorithms I: Fundamentals*, volume 305. Springer science & business media, 1993.
- Sepp Hochreiter. Untersuchungen zu dynamischen neuronalen netzen. *Diploma, Technische Universität München*, 91(1), 1991.
- Sepp Hochreiter and Jürgen Schmidhuber. Long short-term memory. *Neural Computation*, 9(8):1735–1780, 1997.
- Gao Huang, Zhuang Liu, Laurens Van Der Maaten, and Kilian Q Weinberger. Densely connected convolutional networks. In *Proceedings of the IEEE conference on computer vision and pattern recognition*, pages 4700–4708, 2017.
- Sergey Ioffe and Christian Szegedy. Batch normalization: Accelerating deep network training by reducing internal covariate shift. In *International Conference on Machine Learning*, pages 448–456. pmlr, 2015.
- Diederik P Kingma and Jimmy Ba. Adam: A method for stochastic optimization. *arXiv preprint arXiv:1412.6980*, 2014.
- Alex Krizhevsky, Geoffrey Hinton, et al. Learning multiple layers of features from tiny images. 2009.
- Puya Latafat, Andreas Themelis, Masoud Ahookhosh, and Panagiotis Patrinos. Bregman finito/miso for nonconvex regularized finite sum minimization without lipschitz gradient continuity. *SIAM Journal on Optimization*, 32(3):2230–2262, 2022.
- Yann LeCun, Yoshua Bengio, and Geoffrey Hinton. Deep learning. *Nature*, 521(7553):436–444, 2015.

- Chih-Jen Lin, Ruby C Weng, and S Sathiya Keerthi. Trust region newton methods for large-scale logistic regression. In *Proceedings of the 24th international conference on Machine learning*, pages 561–568, 2007.
- Liyuan Liu, Haoming Jiang, Pengcheng He, Weizhu Chen, Xiaodong Liu, Jianfeng Gao, and Jiawei Han. On the variance of the adaptive learning rate and beyond. *arXiv preprint arXiv:1908.03265*, 2019.
- Ilya Loshchilov and Frank Hutter. Sgdr: Stochastic gradient descent with warm restarts. *arXiv preprint arXiv:1608.03983*, 2016.
- Ilya Loshchilov and Frank Hutter. Decoupled weight decay regularization. *arXiv preprint arXiv:1711.05101*, 2017.
- Haihao Lu. “Relative continuity” for non-Lipschitz nonsmooth convex optimization using stochastic (or deterministic) mirror descent. *INFORMS Journal on Optimization*, 1(4): 288–303, 2019.
- Haihao Lu, Robert M Freund, and Yurii Nesterov. Relatively smooth convex optimization by first-order methods, and applications. *SIAM Journal on Optimization*, 28(1):333–354, 2018.
- D Russell Luke. Phase retrieval, what’s new. *SIAG/OPT Views and News*, 25(1):1–5, 2017.
- Liangchen Luo, Yuanhao Xiong, Yan Liu, and Xu Sun. Adaptive gradient methods with dynamic bound of learning rate. *arXiv preprint arXiv:1902.09843*, 2019.
- Nikolay Manchev and Michael Spratling. Target propagation in recurrent neural networks. *The Journal of Machine Learning Research*, 21(1):250–282, 2020.
- Mary Ann Marcinkiewicz. Building a large annotated corpus of english: The penn treebank. *Using Large Corpora*, 273, 1994.
- Arkadij Semenovič Nemirovskij and David Borisovich Yudin. Problem complexity and method efficiency in optimization. *Wiley Interscience*, 1983.
- Yu Nesterov. Smooth minimization of non-smooth functions. *Mathematical Programming*, 103:127–152, 2005.
- Yurii Nesterov. *Introductory lectures on convex optimization: A basic course*, volume 87. Springer Science & Business Media, 2003.
- Andrew Y Ng. Feature selection, L1 vs. L2 regularization, and rotational invariance. In *Proceedings of the twenty-first International Conference on Machine Learning*, page 78, 2004.
- Alasdair Paren, Leonard Berrada, Rudra PK Poudel, and M Pawan Kumar. A stochastic bundle method for interpolating networks. *Journal of Machine Learning Research*, 23: 1–57, 2022.

- Razvan Pascanu, Tomas Mikolov, and Yoshua Bengio. On the difficulty of training recurrent neural networks. In *International Conference on Machine Learning*, pages 1310–1318. Pmlr, 2013.
- Andrei Patrascu and Ion Necoara. Nonasymptotic convergence of stochastic proximal point methods for constrained convex optimization. *The Journal of Machine Learning Research*, 18(1):7204–7245, 2017.
- Herbert Robbins and Sutton Monro. A stochastic approximation method. *The Annals of Mathematical Statistics*, pages 400–407, 1951.
- R Tyrrell Rockafellar. Monotone operators and the proximal point algorithm. *SIAM Journal on Control and Optimization*, 14(5):877–898, 1976.
- R Tyrrell Rockafellar. *Convex analysis*, volume 11. Princeton university press, 1997.
- R. Tyrrell Rockafellar and Roger J.-B. Wets. *Variational Analysis*. Springer Verlag, Heidelberg, Berlin, New York, 1998.
- Alexander Shapiro, Darinka Dentcheva, and Andrzej Ruszczyński. *Lectures on stochastic programming: modeling and theory*. SIAM, 2021.
- Sima Siami-Namini, Neda Tavakoli, and Akbar Siami Namin. The performance of LSTM and BiLSTM in forecasting time series. In *2019 IEEE International Conference on Big Data*, pages 3285–3292. IEEE, 2019.
- Karen Simonyan and Andrew Zisserman. Very deep convolutional networks for large-scale image recognition. *arXiv preprint arXiv:1409.1556*, 2014.
- Ilya Sutskever, James Martens, George Dahl, and Geoffrey Hinton. On the importance of initialization and momentum in deep learning. In *International Conference on Machine Learning*, pages 1139–1147. PMLR, 2013.
- Marc Teboulle. A simplified view of first order methods for optimization. *Mathematical Programming*, 170(1):67–96, 2018.
- Bokun Wang, Shiqian Ma, and Lingzhou Xue. Riemannian stochastic proximal gradient methods for nonsmooth optimization over the stiefel manifold. *The Journal of Machine Learning Research*, 23(1):4599–4631, 2022.
- Mengdi Wang, Ethan X Fang, and Han Liu. Stochastic compositional gradient descent: algorithms for minimizing compositions of expected-value functions. *Mathematical Programming*, 161:419–449, 2017.
- Yang You, Jing Li, Sashank Reddi, Jonathan Hseu, Sanjiv Kumar, Srinadh Bhojanapalli, Xiaodan Song, James Demmel, Kurt Keutzer, and Cho-Jui Hsieh. Large batch optimization for deep learning: Training bert in 76 minutes. *arXiv preprint arXiv:1904.00962*, 2019.

- Tong Zhang. Solving large scale linear prediction problems using stochastic gradient descent algorithms. In *Proceedings of the twenty-first International Conference on Machine Learning*, page 116, 2004.
- Pan Zhou, Jiashi Feng, Chao Ma, Caiming Xiong, Steven Chu Hong Hoi, et al. Towards theoretically understanding why sgd generalizes better than adam in deep learning. *Advances in Neural Information Processing Systems*, 33:21285–21296, 2020.
- Juntang Zhuang, Tommy Tang, Yifan Ding, Sekhar C Tatikonda, Nicha Dvornek, Xenophon Papademetris, and James Duncan. Adabelief optimizer: Adapting stepsizes by the belief in observed gradients. *Advances in Neural Information Processing Systems*, 33:18795–18806, 2020.